

PETROLOGY, STRUCTURE, AND CORRELATION OF  
THE UPPER PRECAMBRIAN ELY'S PEAK BASALTS

A THESIS  
SUBMITTED TO THE FACULTY OF THE GRADUATE SCHOOL  
OF THE UNIVERSITY OF MINNESOTA

BY  
JAMES A. KILBURG

IN PARTIAL FULFILLMENT OF THE REQUIREMENTS  
FOR THE DEGREE OF  
MASTER OF SCIENCE

MAY, 1972



Frontispiece: View, looking northwest, of Ely's Peak and underlying flows in the southernmost portion of the study area.

## TABLE OF CONTENTS

|   | <u>Page</u> |
|---|-------------|
| Abstract.....   | i           |
| Introduction.....   | 2           |
| Purpose of Investigation.....   | 2           |
| Location.....   | 2           |
| Field and Laboratory Methods.....                                     | 3           |
| Previous Work.....  | 5           |
| Acknowledgments.....  | 6           |
| Geologic Setting.....   | 8           |
| Introduction.....   | 8           |
| Thomson Formation.....  | 9           |
| Nopeming Formation.....   | 10          |
| The Duluth Gabbro Complex.....  | 10          |
| Pleistocene Deposits.....   | 11          |
| Igneous Petrology.....  | 13          |
| Introduction.....   | 13          |
| Criteria For Distinguishing Between Flows..                           | 13          |
| Primary Structures of the Flows.....                                  | 14          |
| Primary Igneous Minerals.....   | 16          |
| Chemical and Physical Characteristics.....                            | 24          |
| Petrography and Alteration.....                                       | 36          |
| Flow A.....   | 37          |
| Flow B.....   | 40          |
| Flow C.....   | 40          |
| Flow D.....   | 44          |
| Flow E.....   | 45          |
| Flow F.....   | 48          |
| Unit G.....   | 49          |
| Flow H.....   | 51          |
| Flows I-P.....  | 56          |
| Mafic Dikes.....  | 57          |
| Diabasic Intrusion.....   | 58          |
| Interflow Sediments.....  | 59          |
| Microgranitic Dikes.....  | 59          |
| Petrographic Description of the Basal<br>Flows on Lucille Island..... | 60          |
| Correlation.....  | 62          |
| Variation Diagrams and Differentiation<br>Trends.....                 | 65          |
| Crystallization History.....  | 66          |
| Parent Magma.....   | 68          |
| Discussion.....   | 71          |
| Metamorphic Petrology.....  | 73          |
| Introduction.....   | 73          |
| Innermost Contact Zone.....   | 74          |
| Middle Contact Zone.....  | 75          |
| Outermost Zone.....   | 75          |

|                       | <u>Page</u> |
|-----------------------|-------------|
| Geologic History..... | 88          |
| Conclusions.....      | 92          |
| Appendix A.....       | 93          |
| References.....       | 95          |

#### LIST OF ILLUSTRATIONS

|  |    |
|--|----|
| Fig. 1 - Location Map.....   | 1  |
| Fig. 2 - Columnar Section of the Ely's<br>Peak Basalts.....                        | 7  |
| Table 1 - Electron Microprobe Results of<br>Analyzed Pyroxenes.....                | 18 |
| Fig. 3 - Pyroxene Quadrilateral.....   | 20 |
| Table 2 - Chemical Analyses of Pyroxenes.....                                      | 22 |
| Table 3 - Chemical Analyses.....   | 25 |
| Table 4 - CIPW Norms.....  | 27 |
| Table 5 - Classification of Ely's Peak Basalts                                     | 28 |
| Fig. 4 - Classification Plots.....   | 29 |
| Table 6 - Chemical Analyses of Porphyritic<br>Flows After Subtraction Calculations | 31 |
| Table 7 - Table of Modes.....  | 32 |
| Table 8 - List of Thin Sections.....   | 34 |
| Fig. 5 - Geologic Sections.....  | 42 |
| Fig. 6 - Photomicrographs.....   | 43 |
| Fig. 7 - Photomicrographs.....   | 46 |
| Fig. 8 - Photomicrographs.....   | 52 |
| Fig. 9 - Photomicrograph.....  | 54 |
| Fig. 10 - Photomicrographs.....  | 55 |
| Fig. 11 - A-F-M Diagram.....   | 63 |
| Fig. 12 - Variation Diagrams.....  | 64 |
| Table 9 - Average Chemical Analyses.....   | 69 |
| Table 10 - Average Chemical Analyses.....  | 72 |
| Fig. 13 - Triangular Diagram.....  | 78 |
| Fig. 14 - Petrogenetic Grid.....   | 81 |
| Fig. 15 - P-T Diagram.....   | 82 |
| Table 11 - Pressure-Thickness Relations.....                                       | 85 |
| Fig. 16 - X-ray Pattern of Wairakite.....  | 94 |

## A B S T R A C T

The Upper Precambrian Ely's Peak basalts crop out in a north-south trending, wedge-shaped belt in the area around Nopeming, southwest of Duluth, Minnesota. These Lower Keweenawan flows overlie the basal Upper Precambrian quartzite in the southwestern portion of the Lake Superior basin. There are at least 20 individual flows with a total thickness of about 1,200 feet. The thickest flow is about 125 feet thick while the thinnest is less than 10 feet thick. Many of the flows show considerable lateral continuity; for example, one flow is traceable for about three miles along strike.

Chemically, there are two main types of flows as classified by MacDonald and Katsura (1964); these are alkali basalts and tholeiite basalts. The alkali basalts, which have a low silica content, are fine-to medium-grained and form flows which vary in thickness from about 15 to just over 100 feet. Plagioclase, small, anhedral olivine pseudomorphs, and actinolite after augite form a subophitic to poikilitic texture. The opaque minerals ilmenite and magnetite form phenocrysts up to 1.5 mm in diameter in some rocks but are usually found as interstitial microlites in the groundmass. Textures and structures within the flows suggest a low viscosity. Structures within these flows include level, ropy surfaces, bent and straight pipe vesicles, straight vesicle cylinders, and vesicular tops. Crude columnar joints were observed in one flow.

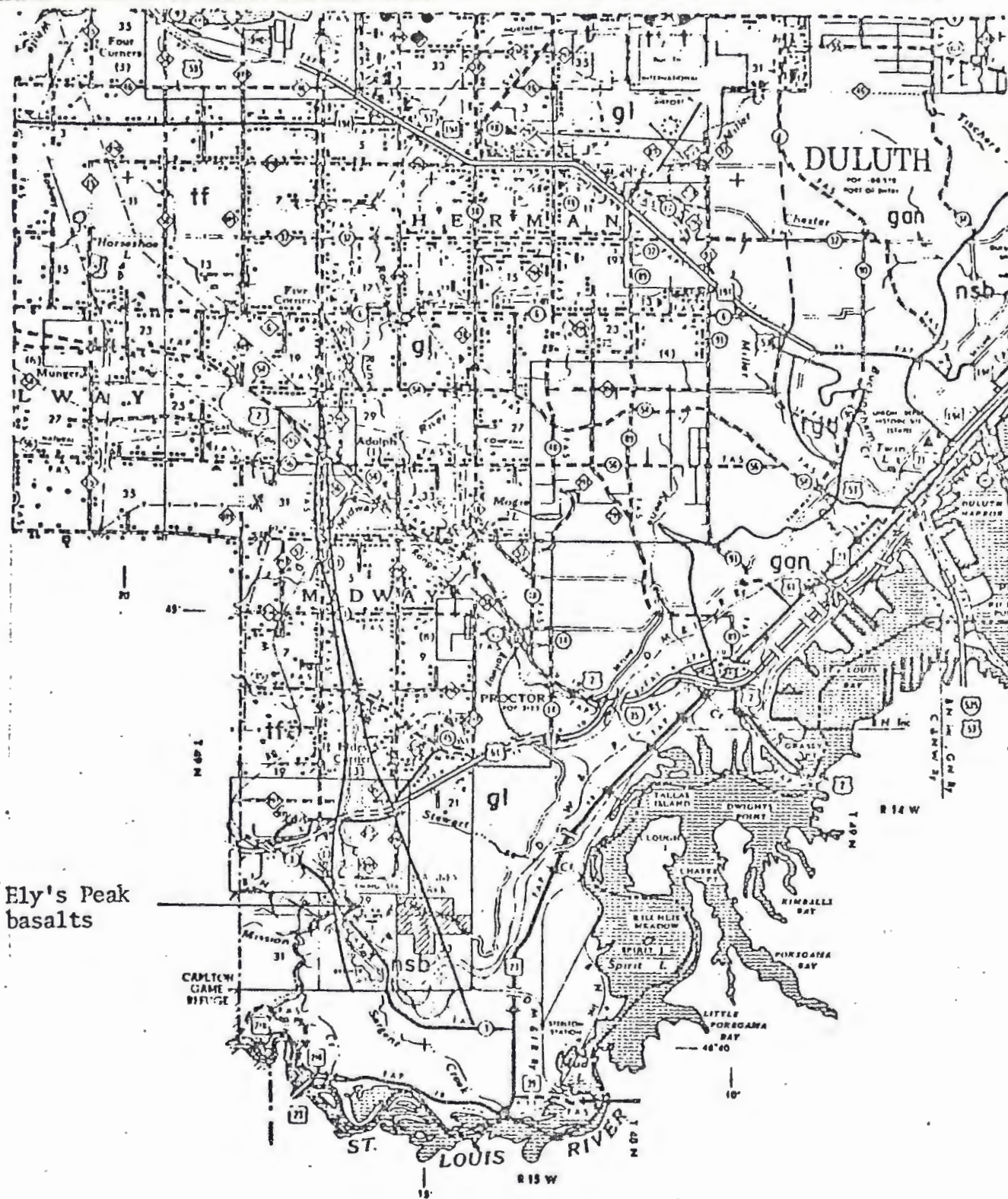
The tholeiitic basalts are usually fine-to medium-grained, but some thicker flows are coarse-grained. These flows are usually from 30 to 90 feet thick. They include porphyritic, subophitic, and poikilitic types. Augite occurs as phenocrysts in the porphyritic flows and as poikilitic oikocrysts and as intergranular grains in the others. Olivine pseudomorphs are occasionally present, and magnetite and ilmenite generally occur as evenly distributed microlites in the groundmass. Structures within the flows include pillows (only in the basal flow), stretched amygdules, and vesicular tops. The augite-porphyritic basalts which lie at the base of the sequence are distinctive and very rare in the North Shore Volcanic Group.

The whole sequence of lavas has undergone hydrothermal metamorphism to the high zeolite-low greenschist facies. Minerals present which demonstrate this are actinolite, chlorite, and epidote. The only zeolite present is wairakite which has been discovered here apparently for the first time in the Lake Superior region. It is the highest-temperature zeolite. Intrusion of the Duluth Complex is thought to be responsible for elevating the geothermal gradient and thus, permitting the formation of wairakite. The gabbro intrusion also contact-metamorphosed the lavas to a medium-grained pyroxene hornfels for a distance of up to one-fifth of a mile from the contact.



Pressures of metamorphism are thought to have been between 2,000 and 2,500 bars. This pressure was produced by the weight of up to 30,000 feet of overlying Upper Precambrian lavas and Duluth Complex which underlie the North Shore of Lake Superior. Temperatures are estimated to have been between 290° C and 370° C during the hydrothermal metamorphism.

Based on their distinctive petrology and reversed magnetic polarity (Green and Books, 1972), the Ely's Peak basalts appear to correlate with the basal flows at Grand Portage, Minnesota. This implies that the time of deposition at these localities was approximately the same, and the source from which these lavas were derived and the physical conditions of magma generation were the same.



**KEY**

- nsb-Ely's Peak Basalts
- gl-Duluth Gabbro Layered Series
- gan-Duluth Gabbro Anorthositic Series
- tf-Thomson Formation

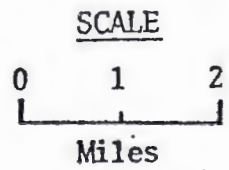


Figure 1 - Map showing location of Ely's Peak basalts.

## INTRODUCTION

### Purpose of Investigation

This study was undertaken to thoroughly characterize the Lower Keweenaw Ely's Peak basalts (Green, 1972), in order to determine the petrogenetic and structural relations at the inception of Keweenaw volcanism in the Duluth area, to provide a basis for lithic correlation, and for interpreting the post-depositional history and environment of these rocks. These basalts are very distinctive mineralogically, because no other flows like them are believed to exist anywhere else above the basal flows in the Lake Superior region. The Ely's Peak basalts are unique because they occupy the base of the igneous pile in the Duluth area and mark the beginning of the igneous activity that occurred in Lower Keweenaw time. Therefore, a knowledge of the petrography, stratigraphy, and structure of the basal flows, and their relationship to overlying flows and associated igneous rocks, is necessary if the igneous history of the entire area is to be well understood.

### Location

The study area is located from less than one mile up to four miles west of the Duluth city limits and is bisected by U. S. Highway 61 (see Figure 1). The area extends from where the unit wedges out three-quarters of a mile north of Adolph southward for about eight miles to where it ends in the Short Line Park area overlooking Fond du Lac and Gary. It is widest at its southern limit, being up to one and one-half miles wide.



The Ely's Peak basalts underlie portions of Sections 29, 30, 31 and 32 of T 50 N, R 15 W; Sections 5, 6, 7, 8, 17, 20, 21, 28, 29, 32 and 33 of T 49 N, R 15 W; and Sections 4 and 5 of T 48 N, R 15 W, St. Louis County, Minnesota.

#### Field and Laboratory Methods

Approximately six weeks were spent in mapping the flows during the summer of 1971. A detailed, flow by flow investigation was carried out where possible; however, this was limited in the central portion of the mapping area due to discontinuity of exposure. Despite this, actual flow by flow mapping was accomplished in the northern part of the study area in the vicinity of the Cloquet water supply tank and in the southern part of the area from Magney Park to the area around Ely's Peak. Where possible, thicknesses of flows were determined by the Brunton and pace method. Where rugged topography limited this method, the flow thicknesses were determined by painstakingly working up steep slopes as nearly perpendicular to strike as possible and counting body lengths all the way up. All of the existing outcrops of the Ely's Peak basalts are believed to have been visited and studied.

Mapping was done on topographic maps at a scale of 1:24,000. The study area covered portions of the Adolph, Esko, and West Duluth U. S. Geological Survey quadrangles. Taylor's geologic map (1964) of the Duluth area was used as a supplement to the topographic maps and was a valuable aid in locating outcrops, as were aerial photographs supplied by J. C. Green. The map presented with this study is at a scale of 1:12,000.

A total of 135 samples of flows and associated rocks were collected during the field work for petrographic study. Forty-three of these samples

were made into thin sections and the writer examined nine more thin sections from J. C. Green's collection. From these 52 thin sections, a detailed petrographic description of the flows was worked out. Six thin sections from the basal flows on Lucille Island near Grand Portage were studied for purposes of comparison and correlation with the flows in the subject area.

Study of the 52 thin sections of the Ely's Peak basalts was done on a Zeiss model KL-18 POL petrographic microscope. Point counts were made for modal analyses with the microscope and point counter by picking a random place to start and then counting the grain which was under the cross hairs after every two clicks of the point counter. A total of 28 thin sections were point counted and 1,000 grains were counted on each section.

Where the feldspars were not badly altered, the method of Michel-Levy was used to determine plagioclase compositions in thin section. Where clouding due to alteration did occur, plagioclase compositions were determined for 15 specimens by using index of refraction oils and the method of Tsuboi. The precision to which these compositions were determined is believed to be within about  $\pm 2\%$  An.

The writer made use of a Picker x-ray diffractometer to identify unknown secondary minerals using a rapid scanning speed of  $4^{\circ}2\theta$  per minute. Approximately 15 minerals were either identified or had their identity confirmed in this way.

The writer also made use of the electron microprobe at the Department of Geology and Geophysics, University of Minnesota, Minneapolis. Seven samples were prepared for study and the writer concentrated on analyzing the pyroxenes. In all, 13 pyroxene grains were analyzed for eight elements and a total of 28 analyses were made (more than one analysis was done on some grains).

### Previous Work

Early geologic reconnaissance in the area was done in 1898 by N. H. Winchell who published a description of the geology and petrography of the flows in the vicinity of Ely's Peak in his 1899 report on the Geology of Minnesota. He largely described the rocks as either trap or gabbroid rocks of the eruptive type. In his publication, Winchell presented a log of a deep well at Short Line Park. The well was drilled in 1888 to a depth of 1,517 feet. The hole went 619 feet into earth, flows, and sandstone before it hit slate, presumably the Thomson Formation.

In 1938, A. E. Sandberg published a strip map of the flows along the North Shore of Lake Superior from Duluth to Two Harbors. His observations of the Ely's Peak basalts were quite brief. He indicated that because of ruggedness of topography and discontinuity of exposure, no flow by flow detail could be worked out. Sandberg distinguished seven flow contacts and estimated that the thickness of flows in the subject area was about 2,500 feet. He suggested that this thickness probably indicated that more than seven flows made up the area.

In 1949, G. M. Schwartz described the geology of the area and included an outcrop map in his report on the geology of the Duluth area. He did not elaborate any more on the number and thickness of flows since Sandberg had worked in the area only ten years before, but he did publish the well log from Short Line Park.

Beginning in 1969, J. C. Green collected samples of several of the flows for petrographic study, made a reconnaissance of the area, and subsequently suggested the Ely's Peak basalts as a thesis problem.

### Acknowledgments

The writer would like to thank Dr. John C. Green, who served as advisor for this study, for his help and generosity, both academic and financial. Financial support for thin sections, chemical analyses, microprobe time, and other items, was provided by the National Science Foundation through research contract No. GA-13411 to J. C. Green.

The writer is also grateful to Dr. James A. Grant, who also served as an advisor and aided the writer in working out the metamorphism of the flows. Thanks also go to the rest of the geology faculty at the University of Minnesota, Duluth, for their help during this study.

Gratitude is also extended to Dr. Paul Weiblen of the University of Minnesota, Minneapolis, who painstakingly taught the writer the use of the electron microprobe.

Special thanks go to Dr. Paul Sims, Director of the Minnesota Geological Survey, for financial support for the field work for this study.

Lastly, the writer would like to thank his wife, Beverly, for supporting him throughout the period of this study and for typing this thesis.



COLUMNAR SECTION OF THE UPPER PRECAMBRIAN  
 ELY'S PEAK BASALTS T48, 49, 50 N, R15 W  
 ST. LOUIS COUNTY, MINNESOTA

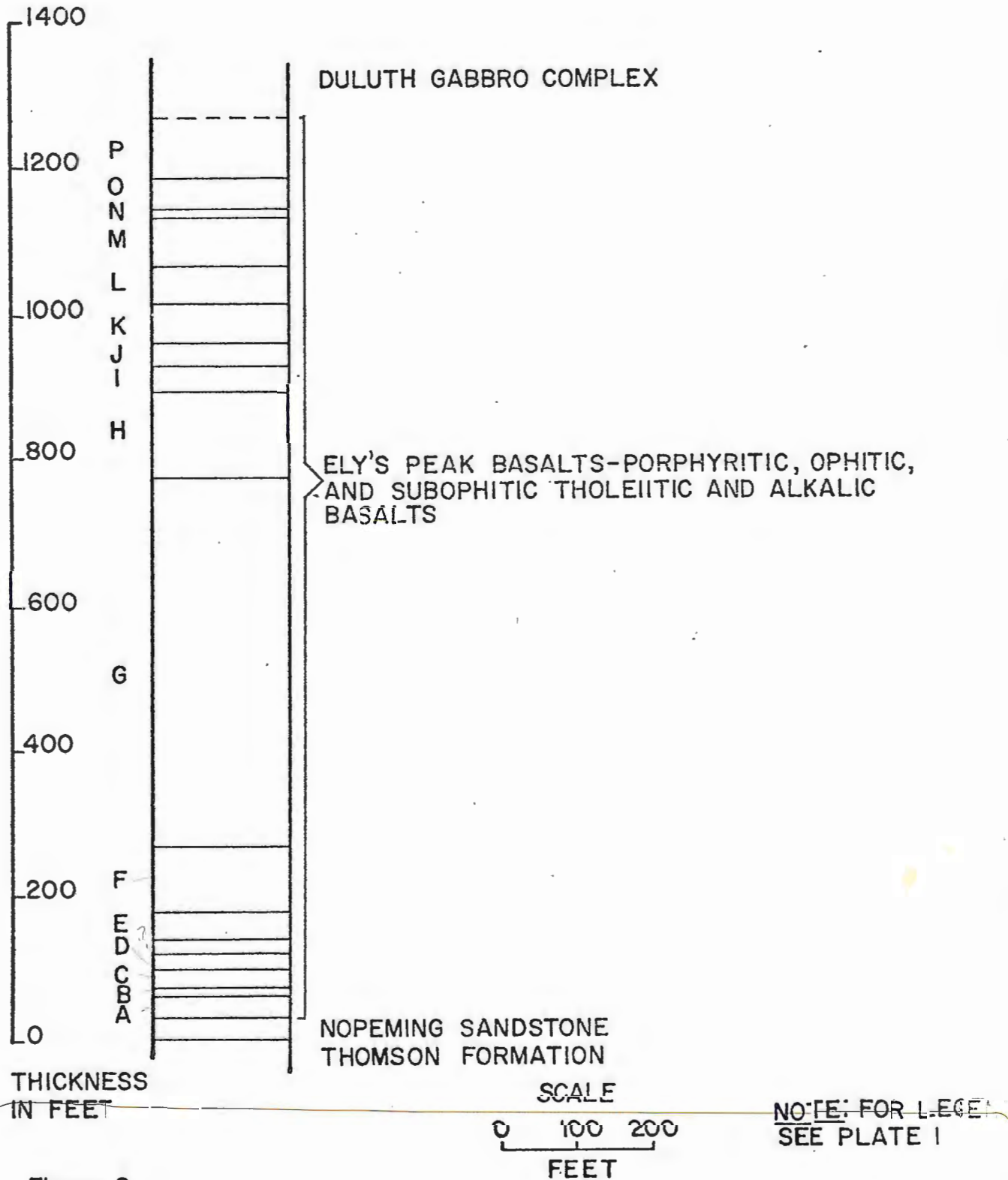


Figure 2

## GEOLOGIC SETTING

### Introduction

The Ely's Peak basalts are a north-south trending, wedge-shaped belt of lava flows approximately eight miles long and up to one and one-half miles wide. They extend from about three-quarters of a mile north of Adolph, T 50 N, R 15 W, to the south where they last occur in the Short Line Park area, T 48 N, R 15 W. At their northernmost extent, the flows pinch out and the Duluth Gabbro Complex nonconformably overlies the Middle Precambrian Thomson Formation. From Adolph to the southern portion of Section 17, T 49 N, R 15 W, there is scant outcrop where no flow by flow stratigraphy could be worked out. South of Section 17 an almost continuous, flow by flow stratigraphy can be determined, except for one large area where outcrop is scarce and flows cannot easily be traced (see map, Plate 1). In this gray area on the map, a thickness of about 500 feet of flows exists in which only three definite flows could be distinguished; however, the thickness suggests that a greater number of flows do exist.

Throughout the entire study area, there is a minimum of 20 flows (see column) with a total thickness of some 1,200 feet. The flows form the basal portion of a great thickness (about 30,000 feet) of lavas which form the northwest limb of the Lake Superior Syncline and are known as the North Shore Volcanic Group (Goldich and others, 1961).

Interflow sediments are very rare in the Ely's Peak basalts. Only three occurrences of sediments were observed and none of these showed any lateral extent; they generally lensed out within a few yards of where they were found.

In the southern portion of the area, the Ely's Peak basalts were intruded by a parallel swarm of basaltic dikes following a joint set that trends about N 30° E. The dikes were eroded more easily than the surrounding extrusive basalts and leave pronounced topographic lineaments in the flows.

On their western margin, the flows conformably overlie the Nopeming Sandstone, which in turn overlies the Thomson Formation at an angular unconformity. To the east, the flows are intersected by the Duluth Complex at an acute angle. To the south and southwest, the flows disappear beneath a thick blanket of Glacial Lake Duluth sediments.

#### Thomson Formation

The western portion of the area is underlain by the Middle Precambrian Thomson Formation. Mapping by Wright, Mattson, and Thomas (1970), and sedimentology studies by Morey and Ojakangas (1970) indicate that the Thomson Formation consists of intercalated metagraywacke, metasilstone, and slate with a total thickness of at least 3,000 feet.

In the subject area, the Thomson Formation is best seen in low road cuts along Midway Road a mile or so to the north of Highway 61, and in a field immediately to the east of Midway Road north of the Grandview Golf Course. In this area, as well as at other locations a few miles to the west, the Thomson Formation has been intensely folded, with fold axes nearly east-west, and dips at high angles to the north and south. Morey and Ojakangas (1970) indicate that the Thomson Formation has undergone metamorphism to the greenschist facies; however, where the Thomson Formation is directly overlain by the gabbro it is contact metamorphosed

to a fine-grained hornfels. To the west, the slates and graywackes disappear under glacial drift, except where exposed in the valley of the St. Louis River.

#### Nopeming Formation

The Nopeming Formation (Mattis, 1972), overlies the Thomson Formation at an angular unconformity and conformably underlies the Ely's Peak basalts. This sandstone unit is at least 25 to 28 feet thick, is buff to light gray in color, cross-bedded, and is a well-indurated quartzite. There is a quartz-pebble conglomerate in a quartzite matrix at the lowest exposed part of the formation.

Mattis' work reveals that the sandstone may have been unconsolidated when the lava flows were deposited on top of it. This idea is based on soft-sediment deformation at the flow/sand contact (where sand has been squeezed up between the basal pillows) and on the pillows in the basal flow overlying the sandstone, indicating that the flows were deposited in water.

The best exposures of the sandstone are along the base of the western hillside to the northwest and southwest of the Cloquet water supply tank, Sections 17 and 20, T 49 N, R 15 W. The actual contact with the flows reveals that the more resistant lavas form overhangs over the sandstone. In its uppermost portions, the sandstone is fine-grained with alternating light and dark bands.

#### The Duluth Gabbro Complex

At their easternmost extent, the Ely's Peak basalts are overlain by the Duluth Gabbro Complex. This Complex has been described by Taylor



(1964) in the Duluth area as a sill-like igneous body, dominantly gabbroic in composition. The rocks are of two main types, each representing a different major period of intrusion. The older gabbro is anorthositic while the younger one is a layered, troctolitic gabbro. In the study area, the rocks immediately adjacent to the basalts belong to the layered series. At the contact with the gabbro, the basalt is completely recrystallized to a fine-grained hornfels. The gabbro is fine-to medium-grained, diabasic olivine gabbro lacking any visible layered structure. Also present in the flows near the contact is a basic pegmatite intrusion containing augite phenocrysts up to six inches long. Taylor has named this pegmatite the Bardon's Peak Intrusion.

Within about 600 feet of the contact along the Duluth, Winnipeg, and Pacific railroad tracks, there appears to have been a good deal of shearing. This is noted by rubbly, brecciated zones cross cutting the flows and intrusion of thin adamellite dikes parallel to these breccia zones, and Taylor suggests that the intrusive basic pegmatites also contained zones of weakness into which independent bodies later intruded.

#### Pleistocene Deposits

In the southwest portion of the area, the flows are overlain by a thick cover of reddish-brown clay from Glacial Lake Duluth (Schwartz, 1949). This clay can best be seen in Sargent and Mission Creeks and their tributaries, where the clay has been deeply eroded by these streams.

In the northern portion of the subject area, the topography consists of swamps and low, rolling hills. Here, glacial drift forms a thin cover on the rock surface. Most of the area is a belt of ground moraine deposited by the Superior Lobe during the last glaciation. One gravel pit

in the southern portion of Section 29 exposes sorted glacial sediments that might represent a former shoreline of Glacial Lake Duluth.

## IGNEOUS PETROLOGY

### Introduction

The Ely's Peak basalts form the basal portion of the North Shore Volcanic Group, which has generally been considered to be made up largely of flood basalts (Turner and Verhoogen, 1960). Since the basal flows have never before been mapped or described in detail, it remains to be seen whether their characteristics fit those of flood basalts. Flow types must be considered, and comparison with flows elsewhere should be attempted before such a classification is given. What follows will be a general description of the structure, petrology, and chemical nature of the flows. A detailed description of the individual flows will also be presented so that they may be thoroughly characterized, classified, and compared with flows elsewhere in the Lake Superior district. Finally, this section will also deal with the differentiation trends, crystallization history, and the parent magma from which the Ely's Peak basalts were derived.

### Criteria For Distinguishing Between Flows

In general, the most often used criterion for distinguishing between successive flows is the presence of a rubbly, amygdaloidal flow top. This top passes downward into a more massive, uniform, crystalline interior and a slightly amygdaloidal base. Not all flows show the rubbly top, but all flows are amygdaloidal in their uppermost portions. Another criterion is that where a series of flows exist, they commonly

form a terraced, erosional surface. Because the upper portions of the flows are amygdaloidal, they erode more easily and form the bench portion while the more resistant massive interior forms the steep portion of the terrace. Other criteria for distinguishing between flows include pipe amygdules at the base of flows and flow surfaces such as ropy surfaces (observed in only one outcrop), lobes, and interflow sediments.

Lithologic changes are occasionally used to distinguish between flows, and care was exercised when these changes were used. For example, on the hillside west of the Cloquet water supply tank where outcrop is discontinuous, if the rock type passed from a porphyritic one to a non-porphyritic one, then a flow contact was considered to have been crossed. In one plagioclase porphyritic flow, it is believed that the phenocrysts settled out in the lava, thereby yielding a flow with more abundant plagioclase phenocrysts at the base than at the top. From this it could be discerned whether a flow contact with the overlying or underlying flow was nearby.

Where flow contacts are vague or subtle, i.e. no rubbly or amygdaloidal tops, a problem arises in trying to differentiate between contacts of individual flows and lithologically similar flows which were extruded in rapid succession to form a flow unit. Where this was encountered, it was assumed that if chilled contacts were well developed, then two individual flows were present. If there was a lack of chilled contacts, then a flow unit was probably present.

#### Primary Structures of the Flows

Pillows: The basal flow is the only pillowed flow. The best exposures of the pillows can be seen near the base of the hillside west and north-



west of the Cloquet water supply tank (SW 1/4, Sec. 17 and NW 1/4, Sec. 20, T 49 N, R 15 W). These pillows are crudely ellipsoidal and measure a foot or two at their longest dimension. They have chilled, vesicular rinds up to a half inch wide. The pillows probably formed in water on the as yet unconsolidated Nopeming Sandstone. Mattis (1972) believes that the Nopeming Sandstone was unconsolidated when the flows were deposited. He bases this on soft-sediment structures and sand squeezed up between the pillows.

Pipe Vesicles: At some locations where the flow bases are exposed, pipe amygdules are present. These are up to 6 inches long and 1/4 inch in diameter. In general, the pipe amygdules are straight, but in some outcrops they are bent. Flow direction could be measured from the unambiguously bent pipes; the direction, based on only three measurements, was to the southeast. Where "ambiguous" bent pipe amygdules occur, they are usually bent in more than one direction.

Vesicle Cylinders: Only one occurrence of vesicle cylinders was found (NE 1/4, SE 1/4, Sec. 29, T 49 N, R 15 W). They were approximately an inch or two in diameter and were tilted to the northeast, perpendicular to the contact.

Ropy and Wavy Surfaces: Ropy surfaces were encountered at two locations. The first location was in the Arrowhead Blacktop Quarry (NW 1/4, Sec. 33 and NE 1/4, Sec. 32, T 49 N, R 15 W), and the second occurrence was below the Duluth, Winnipeg, and Pacific railroad tracks northwest of the railroad tunnel (SW 1/4, Sec. 33, T 49 N, R 15 W).

One wavy surface was observed in outcrop along the railroad tracks south of the trestle at the Arrowhead Blacktop Quarry (SW 1/4, Sec. 33, T 49 N, R 15 W). At this location, the surface looks like rounded,

symmetrical current ripple marks or rug wrinkles about two inches wide. They occur as a cast on the sole of the overlying flow. The flow direction implied here was either north or south.

Stretched Amygdules: At a few locations, stretched amygdules are preserved at the tops of flows. These amygdules are usually a half inch or less in diameter and one or two inches long. They are generally stretched in an easterly or westerly direction, but no statistical study was made.

Columnar Joints: Columnar joints were observed at only one outcrop in the NW 1/4, Sec. 28, T 49 N, R 15 W. They are the normal colonnade type described by Swanson (1967), and appear near the base of the flow in Unit G. They are about 3 feet in diameter and up to 15 feet long. The axis of the columnar joints plunges at about 70° to the southwest and the joints are perpendicular to the flow contact.

### Primary Igneous Minerals

The characteristics of the minerals are constant enough throughout the flows so that general descriptions of the individual minerals can be given apart from their occurrences in specific flows.

Plagioclase: Plagioclase is the dominant mineral in all of the non-porphyritic flows and makes up from about 28% to 55% of the rocks. Size of the crystals varies as flow thickness varies; larger grains are found in thicker flows. A size range of about 0.5 mm to 1 mm in length is common in non-porphyritic rocks. In one plagioclase-porphyritic flow, some of the plagioclase phenocrysts are as much as 8 mm in diameter. No zoning was found in any of the plagioclase but albite twinning is very

common and Carlsbad twinning less common. Combined albite-Carlsbad twins are also occasionally present.

In nearly all instances, the plagioclase has been hydrothermally altered and appears dusty in thin section. Those rocks in which the plagioclase is fresh and clear were collected closer to the contact with the Duluth Gabbro and, therefore, are assumed to have been re-crystallized. In such specimens, the plagioclase has typically lost its original grain boundaries but still occurs as elongate laths.

Since the plagioclase is commonly altered, thereby obscuring twin planes and making the Michel-Levy method unuseable, compositions were determined by index of refraction using the method of Tsuboi (Heinrich, 1965). Where alteration was not so severe as to obscure twin planes, the Michel-Levy method was used as well to determine compositions. Both methods gave plagioclase compositions ranging from about An<sub>28</sub> to An<sub>52</sub>. In general, the dusty plagioclase is rather uniform in composition (An<sub>28</sub> to An<sub>32</sub>) throughout the flows. Where more calcic plagioclase occurs, it is usually clearer and nearer the contact with the Duluth Complex. Compositions in the dusty and clear plagioclase are inferred to be metamorphic compositions and not original igneous compositions.

Clinopyroxene: Two main types of clinopyroxene are present throughout the flows. The first type is diopsidic augite which occurs as ophitic and subophitic grains in the groundmass and as phenocrysts in porphyritic flows. The other type of clinopyroxene is subcalcic augite, which occurs only as subophitic and ophitic grains.

Electron microprobe analysis was done on clinopyroxene phenocrysts and some groundmass clinopyroxene, and the resulting compositions obtained are presented in Table 1 and plotted on the pyroxene quadrilateral

ELECTRON MICROPROBE RESULTS OF ANALYZED PYROXENES

|                                | N-1<br>2<br><u>PT-1</u> | N-1<br>2<br><u>PT-2</u> | N-1<br>2<br><u>PT-3</u> | N-1<br>2<br><u>PT-4</u> | N-1<br>2<br><u>PT-5</u> | N-1<br>1<br><u>PT-1</u> | N-1<br>1<br><u>PT-2</u> | N-4<br>1<br><u>PT-3</u> | N-4<br>1<br><u>PT-4</u> | N-4<br>1<br><u>PT-6</u> | N-4<br>1<br><u>PT-7</u> | N-29<br>1<br><u>PT-1</u> | N-29<br>1<br><u>PT-2</u> | N-29<br>1<br><u>PT-3</u> |
|--------------------------------|-------------------------|-------------------------|-------------------------|-------------------------|-------------------------|-------------------------|-------------------------|-------------------------|-------------------------|-------------------------|-------------------------|--------------------------|--------------------------|--------------------------|
| SiO <sub>2</sub>               | 50.98                   | 52.79                   | 50.99                   | 51.80                   | 49.18                   | 53.17                   | 53.18                   | 52.69                   | 52.38                   | 52.78                   | 52.30                   | 52.95                    | 52.79                    | 51.62                    |
| Al <sub>2</sub> O <sub>3</sub> | 2.46                    | 2.82                    | 2.39                    | 3.44                    | 2.77                    | 2.78                    | 2.86                    | 2.45                    | 2.40                    | 2.31                    | 1.76                    | 3.10                     | 3.06                     | 2.08                     |
| CaO                            | 18.66                   | 18.44                   | 18.39                   | 19.08                   | 18.40                   | 18.54                   | 17.47                   | 17.87                   | 19.12                   | 18.00                   | 19.80                   | 18.58                    | 18.58                    | 18.91                    |
| MgO                            | 18.90                   | 19.25                   | 18.95                   | 17.27                   | 18.94                   | 19.30                   | 19.39                   | 17.67                   | 16.66                   | 15.36                   | 16.45                   | 18.33                    | 18.98                    | 18.05                    |
| FeO                            | 4.58                    | 4.41                    | 4.57                    | 4.53                    | 4.60                    | 4.65                    | 4.40                    | 4.35                    | 4.82                    | 5.47                    | 8.02                    | 4.62                     | 4.70                     | 5.08                     |
| TiO <sub>2</sub>               | 0.63                    | 0.71                    | 0.97                    | 0.90                    | 0.95                    | 0.68                    | 0.98                    | 0.56                    | 0.42                    | 0.55                    | 0.36                    | 0.80                     | 0.49                     | 1.02                     |
| MnO                            | 0.18                    | 0.19                    | 0.19                    | 0.20                    | 0.16                    | 0.22                    | 0.17                    | 0.14                    | 0.03                    | 0.04                    | 0.02                    | 0.18                     | 0.18                     | 0.17                     |
| Na <sub>2</sub> O              | <u>0.25</u>             | <u>1.52</u>             | <u>4.31</u>             | <u>np</u>               | <u>np</u>               | <u>np</u>               | <u>np</u>               | <u>0.09</u>             | <u>0.10</u>             | <u>1.55</u>             | <u>0.15</u>             | <u>np</u>                | <u>np</u>                | <u>2.03</u>              |
| TOTAL                          | 96.64                   | 99.83                   | 100.76                  | 97.22                   | 95.00                   | 99.34                   | 98.45                   | 95.82                   | 95.93                   | 100.06                  | 98.86                   | 98.56                    | 98.78                    | 98.96                    |
| <u>Flow No.</u>                | <u>C</u>                | <u>C</u>                | <u>C</u>                | <u>C</u>                | <u>C</u>                | <u>C</u>                | <u>C</u>                | <u>F</u>                | <u>F</u>                | <u>F</u>                | <u>F</u>                | <u>A</u>                 | <u>A</u>                 | <u>A</u>                 |
| Molar Wo                       | 39                      | 37                      | 38                      | 41                      | 39                      | 37                      | 36                      | 39                      | 41                      | 41                      | 40                      | 39                       | 38                       | 39                       |
| Molar En                       | 53                      | 55                      | 54                      | 51                      | 53                      | 55                      | 56                      | 54                      | 50                      | 50                      | 47                      | 53                       | 54                       | 52                       |
| Molar Fs                       | 8                       | 8                       | 8                       | 8                       | 8                       | 8                       | 8                       | 7                       | 9                       | 9                       | 13                      | 8                        | 8                        | 9                        |

Table 1



ELECTRON MICROPROBE RESULTS OF ANALYZED PYROXENES

| O                              | N-29        | N-29        | N-29        | N-93        | N-93        | N-93        | N-93        | N-93        | N-93        | N-93        | ES-10       | ES-10       | ES-10       | ES-10       |
|--------------------------------|-------------|-------------|-------------|-------------|-------------|-------------|-------------|-------------|-------------|-------------|-------------|-------------|-------------|-------------|
|                                | 2           | 2           | 2           | 1           | 1           | 1           | 2           | 2           | 2           | 2           | 1           | 1           | 1           | 1           |
|                                | <u>PT-1</u> | <u>PT-2</u> | <u>PT-3</u> | <u>PT-1</u> | <u>PT-2</u> | <u>PT-3</u> | <u>PT-1</u> | <u>PT-2</u> | <u>PT-3</u> | <u>PT-4</u> | <u>PT-1</u> | <u>PT-2</u> | <u>PT-3</u> | <u>PT-4</u> |
| SiO <sub>2</sub>               | 52.77       | 53.53       | 53.72       | 51.76       | 51.22       | 51.20       | 50.90       | 51.97       | 50.97       | 50.57       | 54.61       | 55.44       | 52.58       | 50.38       |
| Al <sub>2</sub> O <sub>3</sub> | 2.98        | 3.13        | 3.34        | 3.00        | 2.46        | 3.17        | 3.41        | 2.61        | 2.49        | 2.90        | 2.61        | 2.82        | 2.70        | 2.97        |
| CaO                            | 17.34       | 17.45       | 19.67       | 18.56       | 17.43       | 17.40       | 20.78       | 19.68       | 18.23       | 19.97       | 17.65       | 17.17       | 18.82       | 18.37       |
| MgO                            | 19.83       | 19.65       | 18.45       | 19.18       | 18.19       | 19.63       | 18.22       | 19.01       | 17.53       | 18.76       | 16.72       | 17.09       | 15.83       | 18.01       |
| FeO                            | 4.81        | 4.52        | 4.69        | 4.04        | 4.19        | 3.83        | 3.71        | 3.73        | 5.92        | 3.85        | 4.81        | 5.16        | 4.94        | 4.81        |
| TiO <sub>2</sub>               | 0.77        | 0.78        | 0.80        | 0.46        | 0.31        | 0.39        | 0.44        | 0.34        | 0.63        | 0.42        | 0.56        | 0.89        | 0.83        | 0.90        |
| MnO                            | 0.21        | 0.18        | 0.20        | 0.22        | 0.23        | 0.19        | 0.19        | 0.21        | 0.29        | 0.22        | np          | 0.04        | 0.03        | np          |
| Na <sub>2</sub> O              | <u>0.25</u> | <u>np</u>   | <u>np</u>   | <u>np</u>   | <u>np</u>   | <u>0.56</u> | <u>0.32</u> | <u>0.12</u> | <u>0.12</u> | <u>np</u>   | <u>0.24</u> | <u>0.06</u> | <u>0.35</u> | <u>0.44</u> |
| TOTAL                          | 98.96       | 99.24       | 100.87      | 97.22       | 94.03       | 96.37       | 97.97       | 96.67       | 96.18       | 96.69       | 97.20       | 98.67       | 96.08       | 95.88       |
| <u>Flow No.</u>                | <u>A</u>    | <u>A</u>    | <u>A</u>    | <u>G</u>    | <u>G</u>    | <u>G</u>    | <u>G</u>    | <u>G</u>    | <u>G</u>    | <u>G</u>    | <u>A</u>    | <u>A</u>    | <u>A</u>    | <u>A</u>    |
| Molar Wo                       | 35          | 36          | 40          | 38          | 38          | 36          | 42          | 41          | 39          | 41          | 40          | 38          | 42          | 39          |
| Molar En                       | 56          | 56          | 52          | 55          | 55          | 57          | 51          | 52          | 52          | 52          | 52          | 50          | 50          | 53          |
| Molar Fs                       | 9           | 8           | 8           | 7           | 7           | 7           | 7           | 7           | 9           | 7           | 8           | 12          | 8           | 8           |

Table 1 (continued)

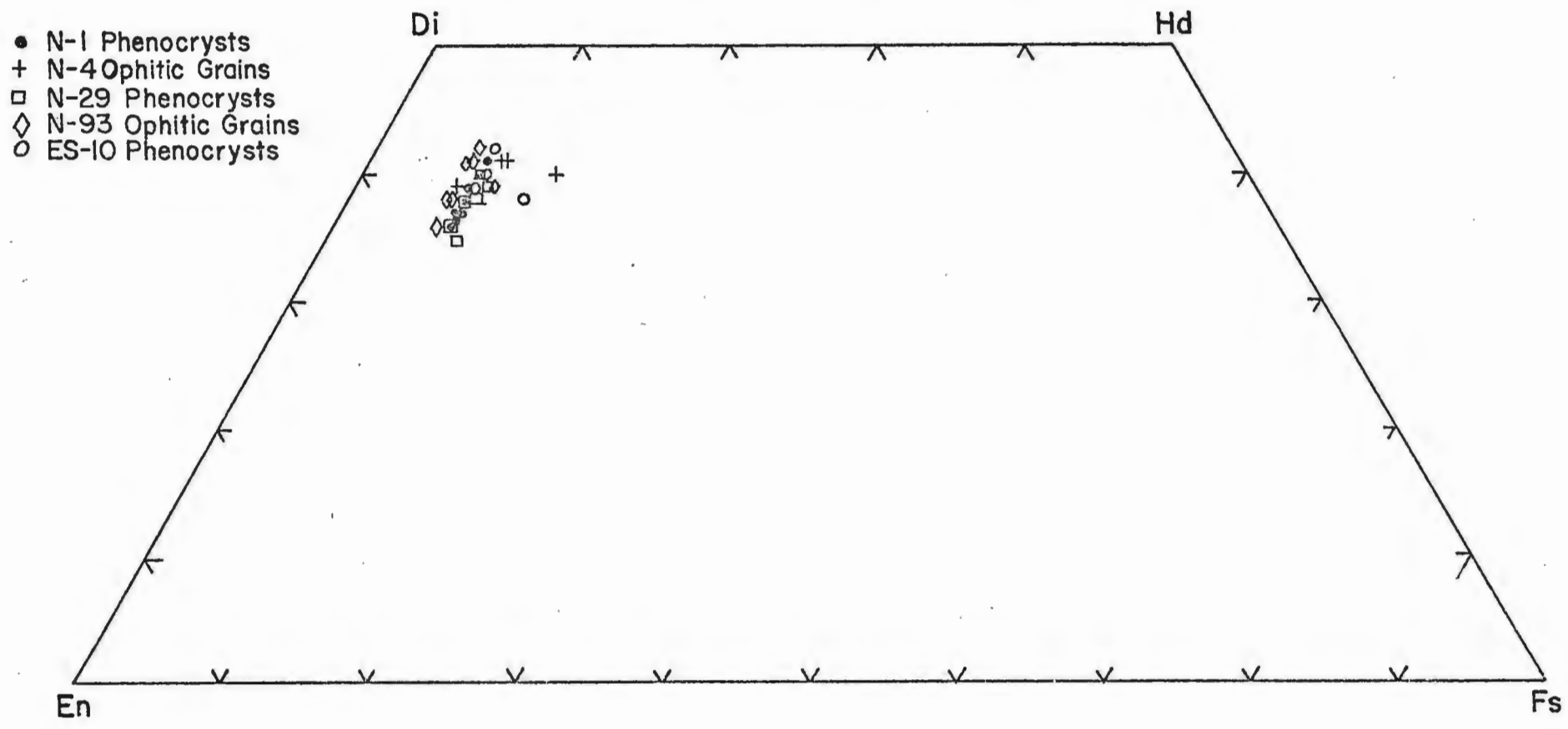


Figure 3: Pyroxene quadrilateral showing compositions determined by the electron microprobe.

in Figure 3. As can be seen from the table and figure, nearly all of the analyzed pyroxenes are of diopsidic augite composition. (No subcalcic augite was analyzed with the electron microprobe). The subcalcic augite was identified by optic axial angles estimated from interference figures. In general, the diopsidic augite appears to have a  $2V$  of about  $40^\circ$  to  $50^\circ$ . The subcalcic augite had optic angles ranging from about  $20^\circ$  to  $40^\circ$ .

In general, the diopsidic augite phenocrysts have concentrically zoned inclusions and occur as single and glomeroporphyritic crystals up to 8 mm in diameter. Electron microprobe analyses of the zoned phenocrysts reveals that composition does not change appreciably from the center to the rim of a crystal. For example, in the first five columns in Table 1, analyses for a traverse across a zoned phenocryst are presented (labeled N-1, 2, points 1 through 5). As can be seen in these columns, there is no appreciable change in chemical composition from point 1, near the center of the crystal, to point 5, near the rim. This visible zoned effect, then, is probably a result only of inclusions incorporated during growth within the individual augite crystals.

In other non-porphyritic flows, diopsidic augite and subcalcic augite form a subophitic to ophitic texture. In some flows, diopsidic augite forms oikocrysts that completely enclose plagioclase. In general, the size of the clinopyroxenes in the groundmass vary according to flow thickness, with larger crystals usually found in flows over 30 feet thick. In many flows, actinolite has almost completely replaced the primary groundmass pyroxene, but some relict scraps are not uncommon.

No pigeonite was detected either as phenocrysts or in the groundmass. If any pigeonite had formed in the groundmass in any of the flows, it has all been altered to actinolite.

As a result of the pyroxene analyses with the electron microprobe, the pyroxenes were found to be rich in magnesia and lime, and poor in iron (see microprobe analyses, Table 1). Chemically, these analyses (see Table 2) are similar to early formed chromian augites from gabbro in the Bushveld Complex and from an olivine pyroxene nodule in melilite basalt from Hofgeismar, Kassel, Germany (Deer, Howie, and Zussman, Vol 2). Since the phenocrysts in the Ely's Peak basalts were not analyzed for chrome, it is not known whether they can be called chromian augites; however, they do compare with these other augites in most other oxide percentages and could contain some chrome. From this, it can be interpreted that the pyroxene phenocrysts in the basal few flows of the Ely's Peak basalts almost certainly formed very early, possibly by fractional crystallization. This is thought to be so because of the relatively high magnesia and lime content and low iron content.

|                                | (1)   | (2)   | (3)   | (4)   |
|--------------------------------|-------|-------|-------|-------|
| SiO <sub>2</sub>               | 52.43 | 52.92 | 52.18 | 47.71 |
| Al <sub>2</sub> O <sub>3</sub> | 4.16  | 2.80  | 2.76  | 12.14 |
| CaO                            | 16.56 | 19.97 | 18.51 | 9.93  |
| MgO                            | 18.19 | 16.40 | 18.20 | 8.24  |
| FeO                            | 3.53  | 5.57  | 4.71  | 10.32 |
| TiO <sub>2</sub>               | 0.37  | 0.50  | 0.66  | 1.88  |
| MnO                            | 0.12  | 0.15  | 0.16  | 0.18  |
| Na <sub>2</sub> O              | 0.96  | 0.35  | 0.73  | 2.68  |
| Cr <sub>2</sub> O <sub>3</sub> | 1.06  | 0.88  | ----  | ----  |
| Fe <sub>2</sub> O <sub>3</sub> | 2.66  | 0.85  | ----  | 2.88  |
| K <sub>2</sub> O               | ----  | ----  | ----  | 0.94  |

Plus other minor oxide components.

Table 2: Chemical analyses of chromian augites from olivine-pyroxene nodule in melilite basalt from Hofgeismar, Kassel, Germany (1); from gabbro, Rustenberg Platinum Mine, Bushveld Complex (2); average of 17 analyses from augite phenocrysts in porphyritic flows from Ely's Peak basalts (3); and average of 8 Ely's Peak basalts (4).

Olivine: Primary olivine is completely absent in any of the flows.

However, olivine pseudomorphs are present in some flows (B, C, D, E, F,



G, H, I, K, L, M, and O) and occur as euhedral to subhedral shapes made of mixtures of serpentine and/or chlorite and possibly bowlingite. The serpentine and chlorite are commonly oxidized to a unusually birefringent type. Occasionally olivine pseudomorphs are rimmed by strings of magnetite and sometimes magnetite forms trains along original fractures through the pseudomorphs.

The olivines which were originally present apparently occurred as small phenocrysts up to 2 mm in diameter in flows G, H, I, K, L, M, and O. In other flows (B, C, D, E, F, and G), smaller olivine pseudomorphs occur as interstitial material and the original olivine may have formed an intergranular texture in the groundmass.

Opagues: Magnetite and ilmenite are the two principal primary opaques in the Ely's Peak basalts. Neither opaque greatly predominates over the other in abundance. In general, magnetite occurs as blocky, subhedral crystals 0.2 to 0.3 mm in diameter. Some magnetite crystals show exsolved ilmenite lamellae. The magnetite is altered nearly everywhere to hematite, and where exsolved ilmenite is present, sphene and hematite occur as alteration products. In many cases, the centers of magnetite crystals alter to hematite before the rims.

Ilmenite occurs as microlites and phenocrysts in flows B, C, D, F, G, H, and L. The ilmenite occurs as thin plates ranging from less than 1 mm to well over 2 mm long. It commonly alters to sphene and in some places to hematite.

Both magnetite and ilmenite show alteration which corresponds to the Class 3 type I of Hubbard and others (1971). This implies hydrothermal alteration at temperatures of about 300° C.

Trace amounts of pyrite and chalcopyrite are disseminated in the flows, but they are most abundant in the Arrowhead Blacktop Quarry (NE 1/4, Sec. 32 and NW 1/4, Sec. 33, T 49 N, R 15 W), where the sulfides occur mainly in veins associated with calcite. William Listerud (personal communication) has identified bornite, chalcocite, and chalcopyrite in one such vein.

Accessory Minerals: Apatite is the most common accessory mineral in the flows and occurs as needle-like prisms in other minerals.

Secondary Minerals: These will be discussed below in the section on metamorphism.

#### Chemical and Physical Characteristics

Table 3 gives new chemical analyses of eight samples of the Ely's Peak basalts, plus one (PP-16) of a similar pyroxene-porphyrific basalt from Lucille Island, near Grand Portage, Minnesota, for comparison, and Table 4 shows CIPW norms. Table 5 gives the classification of the Ely's Peak basalts according to three separate schemes proposed by different petrologists.

According to the classification of Yoder and Tilley (1962), the Ely's Peak basalts would all be tholeiites. Their classification scheme is based on the presence or absence of normative hypersthene. As can be seen by the norms, all of the flows contain normative hypersthene, and, therefore, would be classified as tholeiites, according to Yoder and Tilley.

MacDonald and Katsura's (1964) classification is also shown on Table 5. Their classification is based on a plot of weight percent of total alkalis against weight percent of silica. In Figure 4, the

CHEMICAL ANALYSES OF SELECTED ELY'S PEAK BASALTS

| <u>Sample</u>                  | <u>N-1</u>  | <u>N-4</u>  | <u>N-51</u> | <u>N-89</u> | <u>N-100</u> | <u>N-124</u> | <u>ES-7</u> | <u>ES-10</u> | <u>PP-16</u> |
|--------------------------------|-------------|-------------|-------------|-------------|--------------|--------------|-------------|--------------|--------------|
| SiO <sub>2</sub>               | 47.55       | 50.45       | 49.80       | 45.25       | 45.90        | 49.20        | 45.90       | 47.65        | 48.55        |
| Al <sub>2</sub> O <sub>3</sub> | 6.74        | 13.58       | 11.48       | 15.26       | 15.68        | 13.82        | 12.28       | 8.31         | 9.02         |
| Fe <sub>2</sub> O <sub>3</sub> | 1.37        | 3.54        | 5.89        | 1.82        | 3.88         | 1.72         | 3.34        | 1.49         | 2.63         |
| FeO                            | 11.34       | 8.40        | 7.76        | 10.36       | 8.64         | 10.16        | 14.16       | 11.80        | 10.20        |
| MgO                            | 13.07       | 6.94        | 5.90        | 8.49        | 8.25         | 7.61         | 4.63        | 10.99        | 11.69        |
| CaO                            | 14.21       | 10.13       | 8.02        | 9.58        | 9.77         | 8.66         | 7.26        | 11.84        | 11.29        |
| Na <sub>2</sub> O              | 1.13        | 2.41        | 3.73        | 2.93        | 2.81         | 2.89         | 3.52        | 1.98         | 1.62         |
| K <sub>2</sub> O               | 0.45        | 0.71        | 1.46        | 0.63        | 0.58         | 0.98         | 1.83        | 0.88         | 0.71         |
| H <sub>2</sub> O               | 1.89        | 1.52        | 1.95        | 3.70        | 2.47         | 2.63         | 1.23        | 1.92         | 1.75         |
| CO <sub>2</sub>                | 0.42        | 0.22        | 0.13        | 0.31        | 0.32         | 0.21         | 0.16        | 0.44         | 0.02         |
| TiO <sub>2</sub>               | 1.38        | 1.13        | 2.68        | 0.89        | 0.98         | 1.14         | 4.92        | 1.93         | 1.86         |
| P <sub>2</sub> O <sub>5</sub>  | 0.20        | 0.25        | 0.43        | 0.19        | 0.20         | 0.24         | 0.68        | 0.23         | 0.25         |
| MnO                            | <u>0.20</u> | <u>0.19</u> | <u>0.18</u> | <u>0.16</u> | <u>0.15</u>  | <u>0.16</u>  | <u>0.22</u> | <u>0.19</u>  | <u>0.24</u>  |
| TOTAL                          | 99.95       | 99.57       | 99.41       | 99.57       | 99.63        | 99.42        | 100.13      | 99.65        | 99.83        |

Table 3

Table 3 (continued)

|       |  |
|-------|--|
| N-1   | From Flow C, augite basalt porphyry,<br>SE 1/4, SW 1/4, Sec. 17 of T 49 N, R 15 W.   |
| N-4   | From Flow F, ophitic basalt,<br>NW 1/4, SE 1/4, Sec. 20 of T 49 N, R 15 W  |
| N-51  | From Flow E, plagioclase porphyritic basalt,<br>SE 1/4, SW 1/4, Sec. 20 of T 49 N, R 15 W  |
| N-89  | From Unit G, ophitic basalt,<br>NW 1/4, SW 1/4, Sec. 28 of T 49 N, R 15 W  |
| N-100 | From Flow K, ophitic basalt,<br>SW 1/4, NW 1/4, Sec. 33 of T 49 N, R 15 W  |
| N-124 | From Flow O, subophitic basalt,<br>SE 1/4, SW 1/4, Sec. 33 of T 49 N, R 15 W   |
| ES-7  | From Flow <sup>D<sup>sub</sup></sup> <del>B</del> , subophitic basalt,<br><del>NE</del> 1/4, <del>NW</del> 1/4, Sec. <del>20</del> of T 49 N, R 15 W<br><sub>SE 17</sub> |
| ES-10 | From Flow A; <sup>? <del>sub</del> C</sup> augite porphyritic basalt,<br>NE 1/4, NW 1/4, Sec. 20 of T 49 N, R 15 W   |
| PP-16 | Augite porphyritic basalt from Lucille Island,<br>near Grand Portage, Minnesota  |

Chemical analyses of Ely's Peak basalts were done for this study at the University of Manitoba, Winnipeg, Canada.



CIPW NORMS FOR CHEMICALLY ANALYZED ELY'S PEAK BASALTS

| <u>Sample</u> | <u>N-1</u> | <u>N-4</u> | <u>N-51</u> | <u>N-89</u> | <u>N-100</u> | <u>N-124</u> | <u>ES-7</u> | <u>ES-10</u> | <u>PP-16</u> |
|---------------|------------|------------|-------------|-------------|--------------|--------------|-------------|--------------|--------------|
| Orthoclase    | 2.66       | 4.20       | 8.63        | 3.72        | 3.43         | 5.79         | 10.81       | 5.20         | 4.20         |
| Anorthite     | 14.64      | 25.53      | 12.71       | 28.59       | 30.48        | 23.17        | 13.31       | 13.97        | 15.37        |
| Albite        | 4.56       | 17.77      | 26.97       | 21.10       | 19.96        | 21.95        | 27.88       | 11.51        | 13.47        |
| Quartz        | np         | 4.15       | 3.74        | np          | np           | np           | np          | np           | np           |
| Diopside      | 44.27      | 18.83      | 19.48       | 14.52       | 13.54        | 14.98        | 15.26       | 35.29        | 31.54        |
| Hypersthene   | 17.92      | 19.09      | 10.64       | 0.76        | 9.72         | 19.53        | 4.18        | 15.19        | 19.61        |
| Olivine       | 7.93       | np         | np          | 21.67       | 11.31        | 5.65         | 11.30       | 9.15         | 5.92         |
| Magnetite     | 1.99       | 5.13       | 8.54        | 2.64        | 5.63         | 2.49         | 4.18        | 2.16         | 3.81         |
| Ilmenite      | 2.62       | 2.15       | 5.09        | 1.69        | 1.83         | 2.17         | 9.34        | 3.67         | 3.53         |
| Apatite       | 0.46       | 0.58       | 1.00        | 0.44        | 0.46         | 0.56         | 1.58        | 0.53         | 0.58         |
| Calcite       | 0.96       | 0.50       | 0.30        | 0.71        | 0.73         | 0.48         | 0.36        | 1.00         | 0.05         |

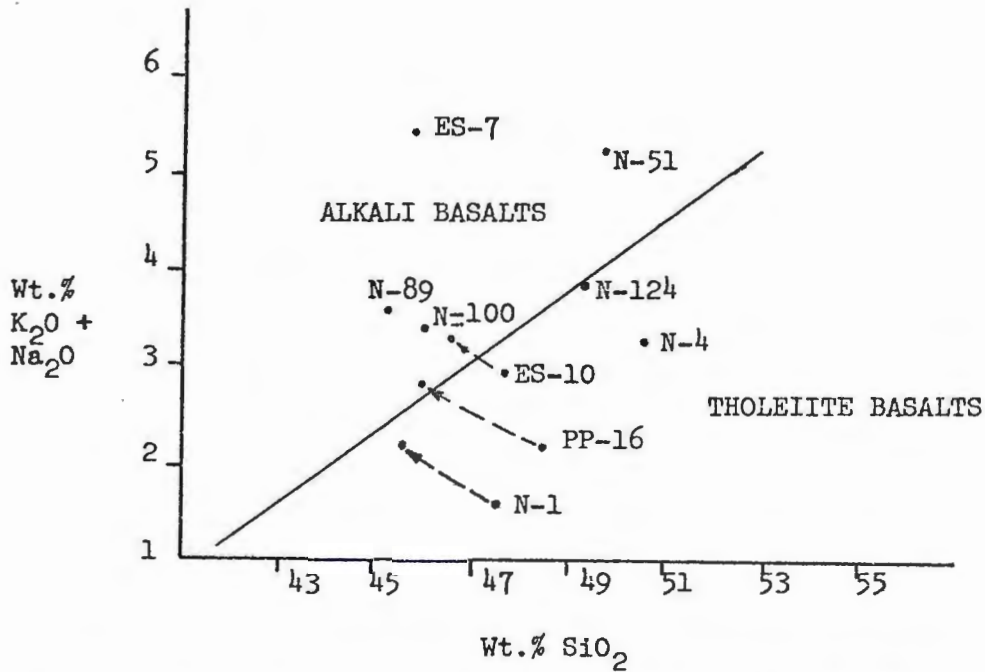
Table 4

CLASSIFICATION OF ELY'S PEAK BASALTS

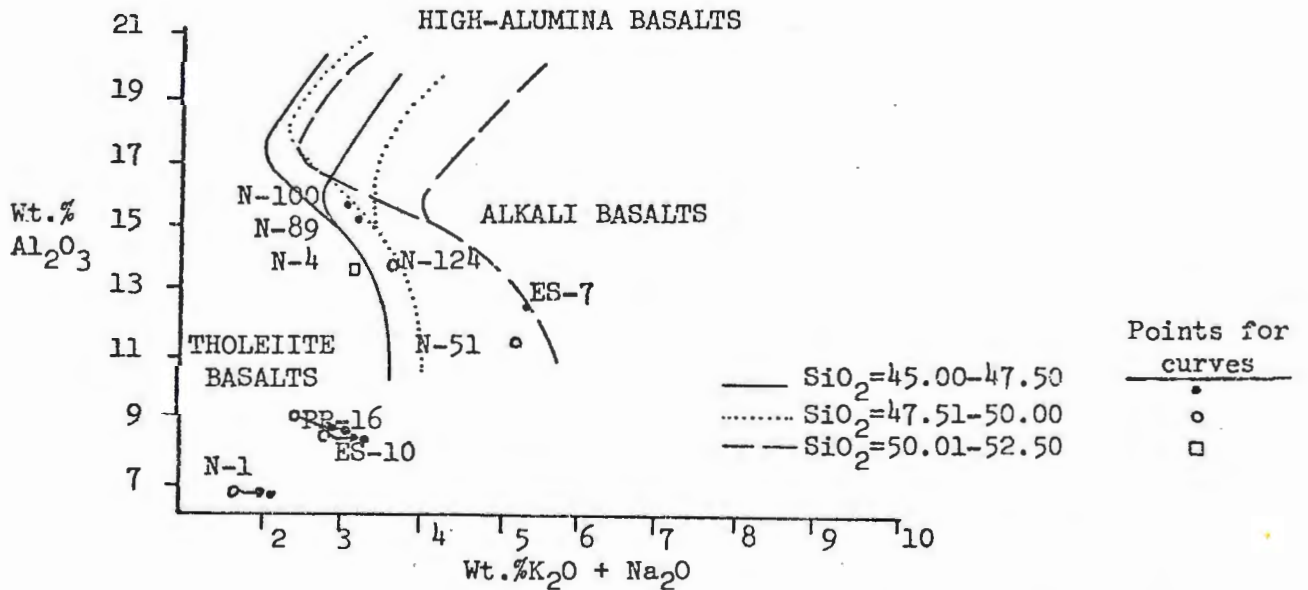
|       | <u>Yoder &amp;<br/>Tilley</u> | <u>MacDonald &amp;<br/>Katsura</u> | <u>Kuno</u>            |
|-------|-------------------------------|------------------------------------|------------------------|
| N-1   | Tholeiite                     | Tholeiite                          | Tholeiite              |
| N-4   | Tholeiite                     | Tholeiite                          | Tholeiite              |
| N-51  | Tholeiite                     | Alkali                             | Alkali Basalt          |
| N-89  | Tholeiite                     | Alkali                             | Alkali Basalt          |
| N-100 | Tholeiite                     | Alkali                             | Alkali Basalt          |
| N-124 | Tholeiite                     | Alkali to<br>Tholeiite             | Alkali to<br>Tholeiite |
| ES-7  | Tholeiite                     | Alkali                             | Alkali                 |
| ES-10 | Tholeiite                     | Tholeiite                          | Tholeiite              |

Table 5

Figure 4



A. MacDonal and Katsura's (1964) plot of total alkalis vs. silica upon which they base their classification of basalts. Compositions of 8 Ely's Peak basalts are plotted in this figure, as is one from flows at Grand Portage, Minnesota(PP-16). ES-10, N-1, and PP-16 are pyroxene-porphyrific flows.



B. Kuno's (1960) plot of total alkalis vs. alumina for three different silica percentages for classification of basalts. Compositions of 8 Ely's Peak basalts are plotted as is one from flows at Grand Portage, Minnesota(PP-16).

compositions of the Ely's Peak basalts are shown on such a plot and they all fall both above and below a diagonal line which divides the figure into two fields; the alkali basalt field above the line and the tholeiitic basalt field below the line. They drew this line by plotting many compositions of Hawaiian basaltic rocks and observing a "clear separation" of rocks that have the respective mineral compositions of the two suites (alkali and tholeiite suites). Therefore, by using this classification, the Ely's Peak basalts appear to belong to both rock suites.

The third classification in Table 5 is that of Kuno (1960). His classification is based on a plot of weight percent of total alkalis against weight percent of alumina for specified ranges of silica weight percentage. Figure 4B is a plot of the compositions of the Ely's Peak basalts using Kuno's parameters. On the graph in Figure 4B, three Y-like curves are plotted, each representing a different silica content. Compositions that plot to the left of the Y curve are tholeiitic; compositions that plot to the right of the Y curve are alkalic; and compositions that plot in the center of the Y are high-alumina basalts. From the compositions plotted on the graph, the Ely's Peak basalts again appear to be of two main types, according to Kuno's curves. These are alkali basalts and tholeiitic basalts.

One other important point is the effect of subtracting the composition of the excess pyroxene phenocrysts from the bulk composition of the rock. Doing this gives a truer picture of the bulk composition of the original rocks if the pyroxene phenocrysts had not crystallized. Subtraction calculations were done on three pyroxene porphyritic flows, two from the Ely's Peak basalts (Flows A and C) and one from the flows



CHEMICAL ANALYSES OF THREE FLOWS  
BEFORE AND AFTER SUBTRACTION CALCULATIONS FOR  
EXCESS PYROXENE PHENOCRYSTS

|                                | <u>PP-16B</u> | <u>PP-16A</u> | <u>ES-10B</u> | <u>ES-10A</u> | <u>N-1B</u> | <u>N-1A</u> |
|--------------------------------|---------------|---------------|---------------|---------------|-------------|-------------|
| SiO <sub>2</sub>               | 48.55         | 46.65         | 47.65         | 46.74         | 47.55       | 45.96       |
| Al <sub>2</sub> O <sub>3</sub> | 9.02          | 8.68          | 8.31          | 8.15          | 6.74        | 6.52        |
| Fe <sub>2</sub> O <sub>3</sub> | 2.63          | 4.68          | 1.49          | 2.15          | 1.37        | 1.33        |
| FeO                            | 10.20         | 9.45          | 11.80         | 11.56         | 11.34       | 10.97       |
| MgO                            | 11.69         | 11.24         | 10.99         | 10.77         | 13.07       | 12.63       |
| CaO                            | 11.29         | 10.86         | 11.84         | 11.61         | 14.21       | 13.74       |
| Na <sub>2</sub> O              | 1.62          | 1.57          | 1.98          | 1.95          | 1.13        | 1.09        |
| K <sub>2</sub> O               | 0.71          | 1.26          | 0.88          | 1.27          | 0.45        | 0.95        |
| H <sub>2</sub> O               | 1.75          | 3.11          | 1.92          | 2.77          | 1.89        | 3.98        |
| CO <sub>2</sub>                | 0.02          | 0.03          | 0.44          | 0.63          | 0.42        | 0.88        |
| TiO <sub>2</sub>               | 1.86          | 1.80          | 1.93          | 1.89          | 1.38        | 1.34        |
| P <sub>2</sub> O <sub>5</sub>  | 0.25          | 0.44          | 0.23          | 0.33          | 0.20        | 0.43        |
| MnO                            | <u>0.24</u>   | <u>0.23</u>   | <u>0.19</u>   | <u>0.18</u>   | <u>0.20</u> | <u>0.18</u> |
| TOTAL                          | 99.83         | 100.00        | 99.65         | 100.00        | 99.95       | 100.00      |

NOTE: "B" after the sample number indicates bulk composition before subtraction, and "A" after the sample number indicates composition after subtraction and recalculation to 100%.

Table 6

TABLE OF MODES

| <u>Sample #</u>             | <u>N-1</u> | <u>N-4</u> | <u>N-8</u> | <u>N-12</u> | <u>N-14</u> | <u>N-23</u> | <u>N-24</u> | <u>N-29</u> | <u>N-38</u> | <u>N-42</u> | <u>N-43</u> | <u>N-55</u> | <u>N-64</u> |
|-----------------------------|------------|------------|------------|-------------|-------------|-------------|-------------|-------------|-------------|-------------|-------------|-------------|-------------|
| <u>Primary Minerals</u>     |            |            |            |             |             |             |             |             |             |             |             |             |             |
| Plagioclase                 | 14.4       | 47.7       | 14.2       | 49.5        | 47.6        | 45.5        | 37.8        | 32.3        | 45.5        | 27.5        | 39.4        | 55.4        | 51.1        |
| Plagioclase                 | np         | np         | np         | np          | np          | np          | np          | np          | np          | 17.6        | np          | np          | np          |
| <u>Phenocrysts</u>          |            |            |            |             |             |             |             |             |             |             |             |             |             |
| Augite                      | 1.2        | np         | np         | 25.3        | 5.6         | 0.8         | 13.3        | 3.9         | 0.9         | 6.8         | np          | np          | 14.3        |
| Augite                      | 53.6       | 25.5       | 40.0       | np          | np          | np          | np          | 19.5        | np          | 12.6        | np          | np          | np          |
| <u>Phenocrysts</u>          |            |            |            |             |             |             |             |             |             |             |             |             |             |
| Ex-Olivine                  | trace      | trace      | trace      | np          | np          | trace       | trace       | trace       | np          | trace       | trace       | np          | 0.6         |
| Magnetite                   | 1.0        | 2.7        | 2.1        | np          | 1.9         | 1.0         | 1.6         | np          | 2.0         | 10.1        | 3.1         | 6.1         | 2.5         |
| Ilmenite                    | 2.1        | 1.0        | 1.0        | 10.2        | 2.0         | 4.1         | 3.6         | 1.7         | 3.1         | 4.1         | 3.2         | np          | np          |
| Apatite                     | np         | np         | np         | 0.2         | trace       | np          | np          | np          | np          | np          | np          | np          | np          |
| Quartz                      | np         | np         | np         | 3.4         | np          | np          | np          | np          | np          | np          | np          | np          | np          |
| <u>Secondary Minerals *</u> |            |            |            |             |             |             |             |             |             |             |             |             |             |
| Actinolite                  | 23.8       | 14.4       | 19.6       | 3.9         | 11.3        | 9.1         | 7.5         | 18.1        | 16.2        | 9.2         | 18.4        | np          | 28.5        |
| Chlorite                    | 2.2        | 7.9        | 3.7        | 4.9         | trace       | np          | np          | 7.9         | 3.3         | 3.1         | 14.6        | 19.5        | np          |
| Epidote                     | np         | np         | np         | np          | np          | np          | np          | np          | 8.7         | 3.8         | 2.7         | 1.3         | 0.2         |
| Calcite                     | np         | np         | np         | np          | np          | np          | np          | np          | 6.1         | np          | 12.9        | np          | np          |
| Sphene                      | 1.7        | np         | np         | np          | np          | 0.5         | 0.4         | np          | 3.9         | 5.2         | np          | 2.0         | np          |
| Hematite                    | np         | np         | np         | np          | np          | np          | np          | np          | 10.0        | np          | np          | np          | np          |
| Adularia                    | np         | np         | np         | np          | np          | np          | np          | np          | 0.3         | np          | 5.7         | np          | np          |
| Quartz                      | np         | 0.8        | 3.6        | np          | np          | np          | np          | np          | np          | np          | np          | 9.3         | 2.6         |
| Biotite                     | np         | np         | np         | 2.6         | np          | 26.0        | 20.8        | 16.7        | np          | np          | np          | 1.2         | 0.2         |
| Hypersthene                 | np         | np         | np         | np          | 30.9        | 10.7        | 8.4         | np          | np          | np          | np          | np          | np          |
| Hornblende                  | np         | np         | np         | np          | 1.7         | 2.3         | 6.6         | np          | np          | np          | np          | np          | np          |
| Matrix Mat'l.               | np         | np         | np         | np          | np          | np          | np          | np          | np          | np          | np          | 5.2         | np          |

\* Secondary minerals include alteration minerals and amygdule minerals.

TABLE OF MODES

| <u>sample #</u>             | <u>N-83</u> | <u>N-85</u> | <u>N-89</u> | <u>N-93</u> | <u>N-100</u> | <u>N-114</u> | <u>N-117</u> | <u>N-118</u> | <u>N-124</u> | <u>ES-3</u> | <u>ES-7</u> | <u>ES-10</u> | <u>PP-14</u> | <u>PP-16</u> |
|-----------------------------|-------------|-------------|-------------|-------------|--------------|--------------|--------------|--------------|--------------|-------------|-------------|--------------|--------------|--------------|
| <u>Primary Minerals</u>     |             |             |             |             |              |              |              |              |              |             |             |              |              |              |
| plagioclase                 | 52.4        | 43.0        | 47.2        | 43.5        | 47.8         | 37.1         | 50.7         | 25.0         | 40.6         | 46.8        | 43.3        | 33.7         | 34.5         | 22.1         |
| augite                      | np          | 12.8        | 13.0        | 23.0        | np           | np           | 30.8         | np           | np           | 16.6        | 15.0        | 5.8          | np           | np           |
| augite                      | np          | np          | np          | np          | np           | np           | np           | np           | np           | np          | np          | 32.5         | 28.9         | 46.0         |
| <u>Phenocrysts</u>          |             |             |             |             |              |              |              |              |              |             |             |              |              |              |
| px-Olivine                  | trace       | np          | 5.0         | trace       | 14.2         | trace        | np           | np           | 14.8         | 9.1         | np          | trace        | 2.4          | 15.1         |
| magnetite                   | 4.0         | 0.1         | 0.9         | 1.7         | 4.2          | 0.3          | np           | 3.5          | 1.0          | 1.3         | 5.6         | 1.9          | 2.0          | np           |
| ilmenite                    | 4.5         | np          | np          | np          | 2.0          | 1.0          | np           | np           | 2.2          | 2.1         | 3.3         | 1.2          | 5.2          | 4.0          |
| quartz                      | np          | np          | np          | np          | np           | np           | np           | 24.3         | np           | np          | np          | np           | np           | np           |
| <u>Secondary Minerals *</u> |             |             |             |             |              |              |              |              |              |             |             |              |              |              |
| actinolite                  | np          | 5.4         | 26.0        | 10.7        | 30.4         | 56.6         | 1.1          | 0.9          | 40.8         | 12.7        | 2.2         | 22.7         | 15.4         | 8.9          |
| chlorite                    | 18.2        | 10.0        | 5.0         | 11.1        | np           | 3.8          | np           | 1.0          | np           | 7.2         | np          | 1.6          | 7.2          | 2.7          |
| epidote                     | 0.1         | 10.9        | np          | 3.9         | np           | 0.1          | np           | np           | np           | 1.8         | np          | 0.6          | 0.1          | np           |
| calcite                     | 0.3         | np          | np          | np          | np           | 0.3          | np           | np           | np           | np          | np          | np           | 0.3          | np           |
| sphene                      | 7.0         | 1.5         | 2.4         | 2.1         | 1.4          | 0.8          | np           | np           | 0.6          | 2.4         | np          | np           | 2.0          | 1.2          |
| hematite                    | np          | 15.0        | np          | np          | np           | np           | np           | np           | np           | np          | np          | np           | np           | np           |
| adularia                    | np          | np          | 0.5         | 0.4         | np           | np           | np           | np           | np           | np          | np          | np           | np           | np           |
| quartz                      | np          | 0.8         | np          | 3.6         | np           | np           | np           | np           | np           | np          | 0.2         | np           | 2.0          | np           |
| biotite                     | 10.4        | np          | np          | np          | np           | np           | np           | np           | np           | np          | 19.5        | np           | np           | np           |
| hornblende                  | 3.1         | np          | np          | np          | np           | np           | np           | 0.2          | np           | np          | 6.8         | np           | np           | np           |
| prehnite                    | np          | 0.5         | np          | np          | np           | np           | np           | np           | np           | np          | np          | np           | np           | np           |
| olivine                     | np          | np          | np          | np          | np           | np           | 17.4         | np           | np           | np          | np          | np           | np           | np           |

\* Secondary minerals include alteration minerals and amygdale minerals.

Table 7 (continued)

LIST OF THIN SECTIONS OF ELY'S PEAK BASALTS AND  
CORRESPONDING FLOWS FROM WHICH THEY WERE MADE

| <u>Flow</u>            | <u>Thin Section No.</u>                                 |
|------------------------|---|
| A                      | N-29, N-38, N-43, ES-10                                 |
| B                      | N-46, N-83, (ES-7) <sup>x</sup>                         |
| C                      | N-1, N-8  |
| D                      | N-23, N-24      ES-7                                    |
| E                      | N-42, N-51, N-53  |
| F                      | N-4, N-47   |
| Unit G                 | N-61, N-62, N-64, N-72, N-75;<br>N-85, N-87, N-89, N-93 |
| H                      | N-131   |
| I                      | N-97, N-129   |
| J                      | N-115   |
| K                      | N-100, N-109  |
| L                      | N-104, N-122  |
| M                      | N-114   |
| N                      | None  |
| O                      | N-124   |
| P                      | N-117   |
| Mafic Dikes            | N-82, N-125   |
| Interflow<br>Sediments | N-49, N-55, N-103                                       |
| Granitic Dike          | N-118   |
| Gabbroic<br>Intrusive  | N-12  |

Table 8



on Lucille Island, near Grand Portage, Minnesota. The results of these calculations are shown in Table 6, along with the bulk rock compositions of the porphyritic rocks. By plotting these recalculated percentages on the figures of Kuno and MacDonald and Katsura, it can be seen that the original composition of the porphyritic rocks changes toward the alkali basalt field in each figure.

The alkali basalts (Flows B, E, G, and K), are fine-to medium-grained and form flows which vary in thickness from about 10 to just over 100 feet. Modal and normative values are listed in Tables 7 and 4 respectively. A key for these tables is shown in Table 8 where the flows are listed together with the representative thin section from each flow. As can be seen in the table of modes, the alkali basalts contain about 43% to 48% plagioclase. Olivine phenocryst pseudomorphs are present as are intergranular olivine pseudomorphs. These, together with actinolite after augite, form subophitic and ophitic textures. Flows over 30 feet thick are usually ophitic, whereas flows under 30 feet thick are commonly subophitic.

Chemical analyses of the alkali basalts (N-51, N-89, N-100 and ES-7) show, with the exception of N-51, a low silica content of about 45% to 46%; and all four of these flows contain between 3% and 5% total alkalis. Structures within these flows include level, ropy surfaces, bent and straight pipe vesicles, straight vesicle cylinders and vesicular tops. These structures and the low silica content suggest a low viscosity of the lavas.

The tholeiitic basalts are generally fine-to medium-grained, but flows over about 50 feet thick are coarse-grained. Most of these flows are between 30 and 90 feet thick. Four flows of this type are chemically

analyzed (Flows A, C, F, and O) and the results are shown in Table 3. It should be noted that two of these four flows are augite porphyritic (Flows A and C). The other two flows are ophitic (Flows F and O). Plagioclase makes up about 19% to 47% of the flows, the porphyritic flows containing less amounts of plagioclase. Except for Flow O, olivine pseudomorphs are not overly abundant in the mode nor is olivine abundant in the norm. Augite occurs as phenocrysts in the porphyritic flows and as oikocrysts in Flows F and O. Magnetite and ilmenite generally occur as evenly distributed microlites in the groundmass.

Chemical analyses of the tholeiitic flows (N-1, N-4, N-124, and ES-10) shows a silica content between 47% and 50% with a total alkali content of between 1% and 4%. Structures within the flows include pillows (only in the basal flow), stretched amygdules, vesicular tops, and perhaps settled-out augite phenocrysts in Flow C. With these structures and the higher silica content, a low viscosity lava is implied.

#### Petrography and Alteration

In general, the Ely's Peak basalts can be divided into two groups of flows. These groups are based on the petrographic nature of the flows and on the stratigraphic position which they occupy. Thus, the first group of flows (A through F on the stratigraphic column in Figure 2) is made up of augite porphyritic flows which occur only at the base of the sequence and make up about 200 feet of the total thickness of all the flows. These flows can be found north of U. S. Highway 61 in the vicinity of the Cloquet water supply tank and south of U. S.

Highway 61 in the area around Nopeming. The second group of flows (G through P on the stratigraphic column in Figure 2) are subophitic and poikilitic basalts which make up the remaining flows of the Ely's Peak basalts and have a total thickness of about 1,000 feet. These flows occur south of U. S. Highway 61 and can best be seen in the area between Magney Park, Short Line Park, and the Arrowhead Blacktop Quarry.

A detailed description of the petrography and alteration will now be presented. Table 8 shows a list of the thin sections studied and the corresponding flows from which they were made. This table can be used as a key to the modal analyses in Table 7.

#### Flow A

Field Observations: Flow A, the basal flow, first crops out north of the Cloquet water supply tank along the hillside east of Midway Road. It conformably overlies the Nopeming sandstone. The flow is traceable to the south along strike for about three-quarters of a mile. It occurs again south of Highway 61 along the Nopeming Road, where it is traceable for about 200 yards. The last occurrence of the flow is in Sargent Creek just west of where it crosses under St. Louis County Highway 3. At this location, about 100 yards of outcrop exists. Only the top of the flow is exposed and it is amygdaloidal and contains stretched amygdules. At this location, the flow is cut by a basaltic dike. It is believed that it is the basal flow that occurs at these latter two locations because it is overlain by a slightly augite porphyritic, fine-grained flow as in the northern portion of the area near the Cloquet water supply tank. Its base, however, is not exposed south of Highway 61.

In the exposures northwest and southwest of the Cloquet water supply tank, the flow is recognized by its conformable contact with the Nopeming Sandstone. The more resistant flow forms overhangs atop the sandstone. The flow is fine-grained, dark gray, porphyritic basalt with small, black, blocky augite and altered olivine phenocrysts. It is about 25 to 30 feet thick and is amygdaloidal in its upper portion.

Structures within the flow include some pipe vesicles and pillows. The pipe vesicles, only at the base, are straight, about 2 to 4 inches long, and are often filled with chlorite. The pillows occur all through the flow and are marked by thin, vesicular rinds about one-half inch thick. They are usually a foot or two across at their longest dimension.

Petrography: Thin sections of the basal flow from north of Highway 61 reveal that the basalt contains about 20% single and glomeroporphyritic, euhedral, zoned augite phenocrysts about 1 to 2 mm in diameter. The augite is commonly twinned with (100) as the twin plane. It is altered along crystal edges, cracks, seams, and zone boundaries to pale green actinolite. Nearly all of the pyroxene in the groundmass (only about 3.5% fresh groundmass augite remains) has been altered to actinolite, which makes up about 18% of the rock.

The plagioclase constitutes about 32% of the rock and occurs as laths less than 1 mm long. It appears fresh, has irregular boundaries, and shows albite twinning. Refractive index determination yields a composition of  $An_{28-32}$ . Some of the plagioclase contains inclusions of actinolite and biotite. In one thin section, the plagioclase is slightly dusty and contains actinolite and chlorite inclusions. The fresh plagioclase with irregular grain boundaries and the high per-



centage of biotite suggest that this flow has undergone some contact metamorphism where it occurs in the northernmost outcrops northwest of the Cloquet water supply tank. Here, it is only about 1,200 feet from the base of the Duluth Complex.

Olivine pseudomorphs are rare in the basal flow, but where they do occur they are composed of chlorite or serpentine and biotite. The pseudomorphs are less than 1 mm in diameter and occur as intergranular microlites. Chlorite occurs as an alteration product of olivine and pyroxene and makes up some 8% of the rock.

In one thin section from the northernmost outcrops northwest of the Cloquet water supply tank, biotite makes up some 17% of the groundmass. It occurs as both interstitial flakes and small clusters of flakes, possibly suggesting alteration of olivine pseudomorphs.

Ilmenite plates up to 0.5 mm long make up about 1% and scraps of magnetite make up about 0.5% of the rock. Small, anhedral masses of sphene are commonly present in the proximity of altered opaques suggesting that the sphene was derived from the opaques. The opaques appear to be altered to the type I alteration described by Hubbard and others (1970). This alteration implies hydrothermal metamorphism of the opaques at temperatures of about 300° C.

A chemical analysis was obtained for sample ES-10 which was taken from this flow, and the results are presented in Table 3. Chemically, this flow is classified as a tholeiitic basalt, based on MacDonald and Katsura's (1964) classification.

### Flow B

Field Observations: Flow B lies stratigraphically above the basal flow and crops out sparsely along the hillside east of Midway Road. Flow B is amygdaloidal in its lowermost 12 inches with chlorite filling the vesicles. The flow is traceable to the south, across Highway 61, where it occurs in one outcrop above the Nopeming Road.

The flow is about 10 feet thick, fine-grained, dark gray, slightly augite-porphyrific basalt with dark green to black patches of chlorite throughout. It is amygdaloidal in its uppermost portions; and near the contact with the Duluth Complex, the flow contains biotite suggesting that the flow is somewhat contact-metamorphosed.

A chemical analysis was obtained for sample ES-7 from this flow, and the results are shown in Table 3. Chemically, this flow is classified as an alkali basalt, based on MacDonald and Katsura's (1964) classification.

### Flow C

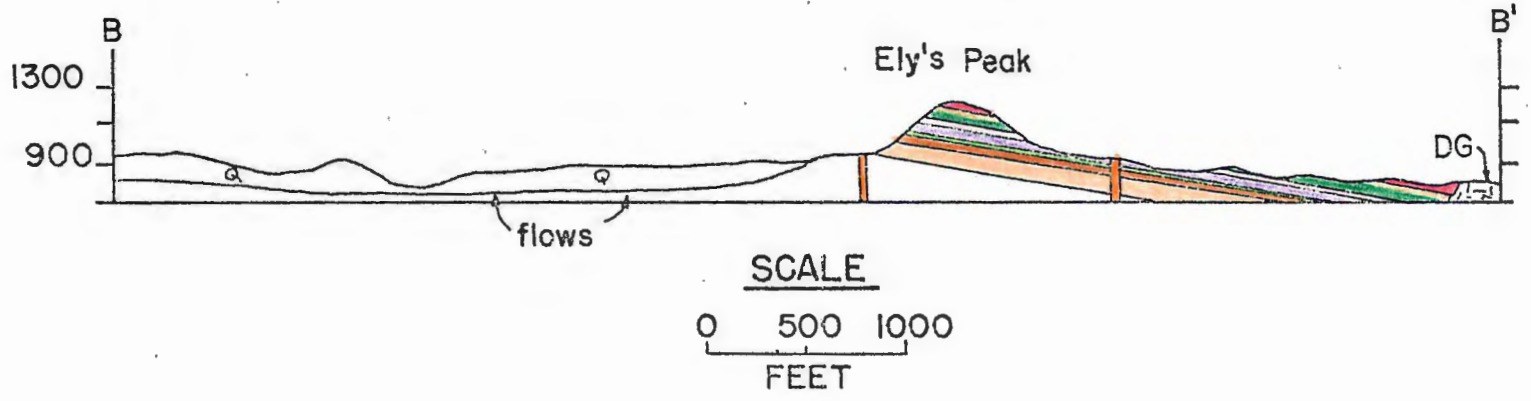
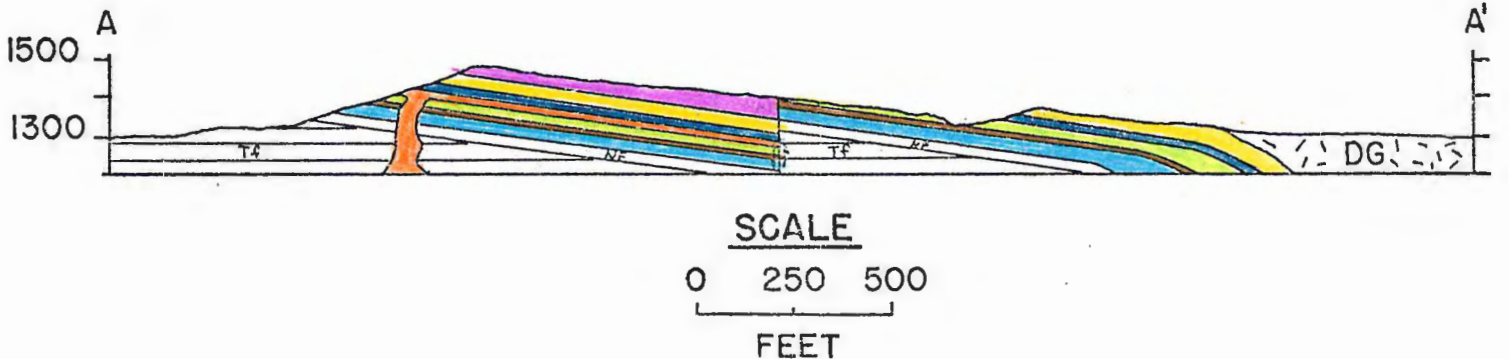
Field Observations: Flow C overlies Flow B but no exposed contact could be found. The flow crops out along the west hillside north of the Cloquet water supply tank, along the fire line just west of the water supply tank, and to the south along the hillside in Sections 17 and 20, T 49 N, R 15 W. The thickness of the flow appears to be about 25 feet. The flow was also encountered on the east hillside about 600 feet east of the water supply tank and again in a cow pasture about one-half mile southeast of the water supply tank. Since the flow dips at about 8 to 10 degrees to the east, it should lie about 150 feet below

where it occurs east of the water supply tank and to the south in the cow pasture. The writer infers that a northeast trending fault may cut the flows with the eastern side as the upthrown block (see map and cross section, Figure 5). A normal stratigraphic sequence exists to the south of Highway 61 where Flow C is found to be in its proper stratigraphic position. Therefore, in order for it to occur north of Highway 61 on the east side of the hill (see cross section), there may be a fault present. If so, it would have to be arcuate, bending from northeast toward the south and then bending back to the southeast.

In the field, Flow C is easily recognized because it is a dark gray, fine-to medium-grained basalt porphyry. Abundant black, blocky, single and glomeroporphyritic augite phenocrysts weather in relief, and the weathered surface is light brown to buff colored due to weathering of feldspars. The augite phenocrysts are larger near the base (up to 8 mm), whereas near the top of the flow they decrease in size to about 3 mm or less. The actual top was not seen.

Petrography: Thin section study of this flow reveals that the augite phenocrysts make up some 54% of the rock, but a range of about 40% to 60% is likely as the 54% is based on only one point count from one thin section. These phenocrysts are euhedral, single and glomeroporphyritic, zoned augites up to 8 mm in diameter (see photomicrograph, Figures 6A and B). They are commonly twinned along the (100) twin plane. Actinolite (which makes up about 23% of the rock), is a common alteration product of augite and occurs along crystal edges, cracks, seams, and zone boundaries. All the clinopyroxene in the groundmass has been altered to actinolite.

GEOLOGIC SECTIONS A-A' & B-B' SHOWING  
 STRATIGRAPHIC RELATIONS OF THE ELY'S PEAK BASALTS

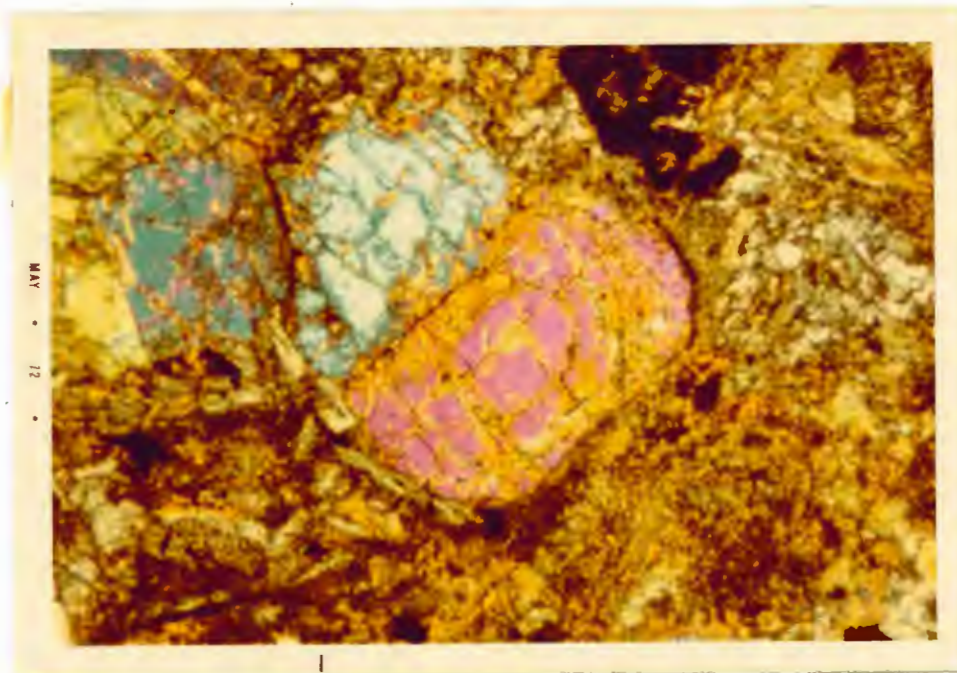


NOTE: FOR LEGEND SEE  
 MAP PLATE I.

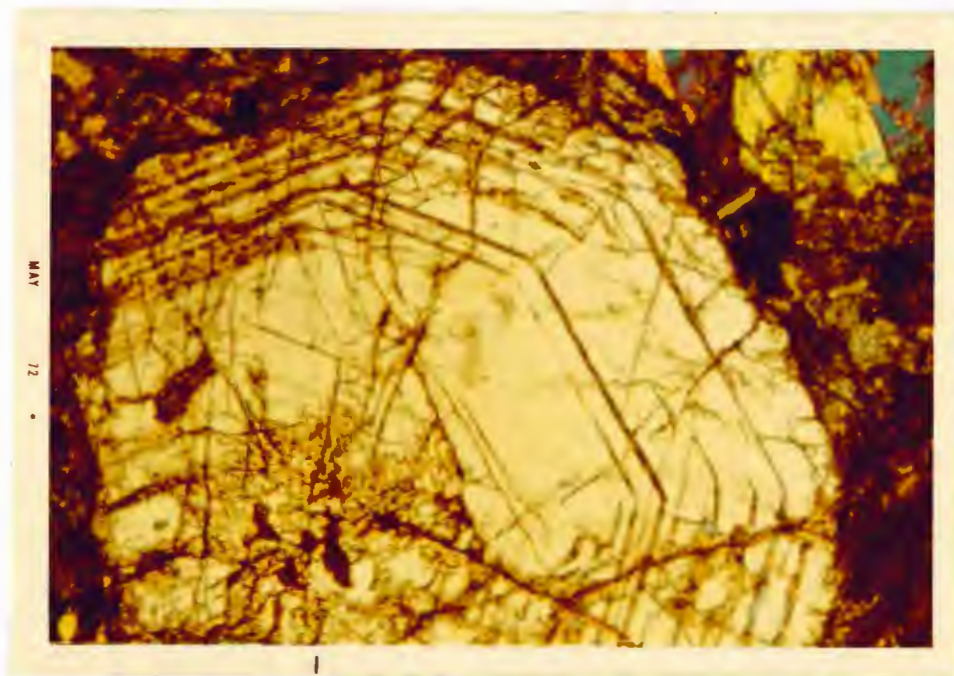
Figure 5

42





A. Photomicrograph showing single, zoned augite phenocryst, from Flow C



B Photomicrograph showing a portion of a zoned augite phenocryst which forms part of a glomeroporphyritic crystal, from Flow C.

1mm

Plagioclase makes up about 15% of the rock and occurs as laths less than a millimeter long. It is dusty and altered to sericite and shows albite twinning; however, sharp twin boundaries have been nearly obliterated due to heavy alteration. No plagioclase compositions were determined because of the alteration.

Ilmenite blades up to 1.5 mm long make up about 2% of the rock and magnetite makes up about 1% of the rock. Both ilmenite and magnetite are highly altered. Sphene (about 2%) is commonly seen near ilmenite whereas hematite occurs inside skeletal magnetite (see photomicrograph, Figure 7A).

Chlorite and clinozoisite make up about 2% of the rock and are alteration products of augite. Near the contact with the Duluth Complex biotite appears. This is typical for all of the flows in the outer zone of contact metamorphism by intrusion of the gabbro.

Some possible olivine pseudomorphs exist but these are rare and only make up one to two percent of the rock.

A chemical analysis was obtained for sample N-1 from this flow, and the results are shown in Table 3. Chemically, this flow is classified as a tholeiitic basalt, based on MacDonald and Katsura's (1964) classification.

#### Flow D

Field Observations: This flow is about 10 feet thick and lies stratigraphically above Flow C. It occurs near all of the same locations as Flow C.

The flow is fine-grained, dark gray, non-porphyrific basalt with dark green to black patches of chlorite throughout. Nearly all of the

augite in this rock has been altered to actinolite. It shows no special characteristics and generally resembles the groundmass of Flow B.

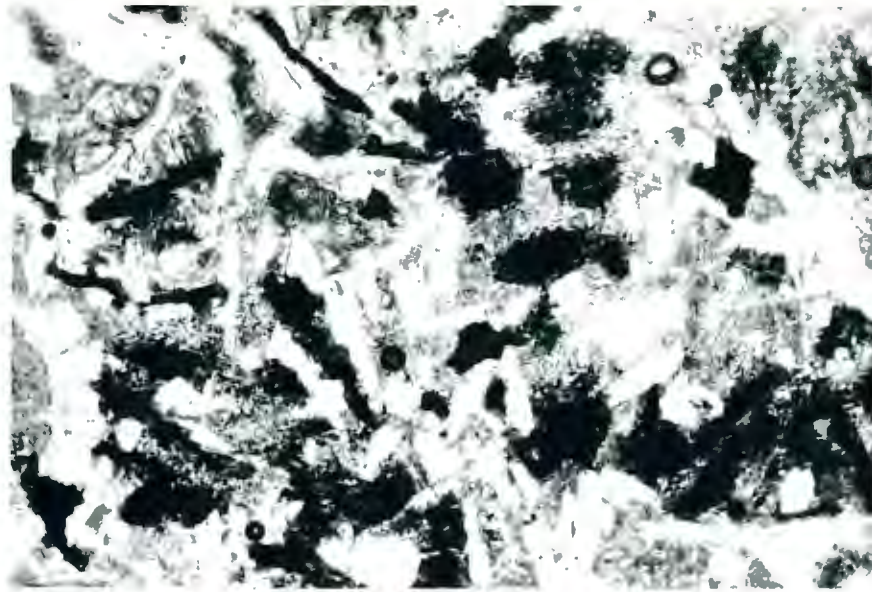
#### Flow E

Field Observations: Flow E is about 30 to 35 feet thick and is not seen in outcrop along the hillside where the Cloquet water supply tank is located but is thought to be present near the top beneath glacial cover. The flow crops out in two locations north of Highway 61, on the upthrown block of the earlier described fault. The flow is also present south of Highway 61, north of the Nopeming Sanatorium.

The first, and northernmost occurrence, is about 700 yards north of the highway in a ravine. The second occurrence is on the western edge of a bluff just to the north of the highway. Here the contact with the overlying flow is well exposed. It also occurs just south of Highway 61 along an east-west trending hillside. This is probably the best exposure of the flow. Both the top and bottom portions are clearly visible. The southernmost outcrop is along a heavily wooded hillside about 2,000 feet southeast of the Nopeming Sanatorium. Flow E is amygdaloidal at its top with chlorite, epidote, and adularia filling the vesicles. The base of the flow contains pipe vesicles filled with adularia and the top is very amygdaloidal.

The flow is fine-grained, dark gray, plagioclase-porphyrific basalt (see photomicrograph, Figure 7B) with occasional augite phenocrysts. The plagioclase is orange and platy and there is a noticeable difference in abundance from the base to the top of the flow. There is much less plagioclase, and the crystals are smaller near the top of the





A. Photomicrograph showing ilmenite plates and magnetite blocks altering to sphene and hematite, from Flow B.



B. Photomicrograph showing a portion of plagioclase phenocrysts that occur in Flow E.

1mm

flow while tablets up to one-half inch in diameter occur in the middle and basal portions of the flow, suggesting settling.

Petrography: Single and glomeroporphyritic augite phenocrysts up to 2 mm in diameter make up about 13% of the rock. The augite is altered to actinolite and biotite.

Plagioclase phenocrysts make up about 18% near the middle of the flow (Figure 7B). They are dusty and altered to sericite. Index of refraction studies yield a composition of  $An_{30-32}$  and this is verified by the Michel-Levy method. Crystal size reaches a maximum of about 8 mm in diameter for plagioclase tablets and slightly over 1 mm in thickness. In addition to containing diopside inclusions, there are often inclusions of magnetite in the plagioclase.

A few pseudomorphs of olivine are present in the thin section but they probably do not make up more than 1% of the rock.

The groundmass is very dusty and composed of plagioclase (28%), magnetite (10%), actinolite (9%), and augite (7%). Some of the plagioclase is clear but much of it contains hematite dust. Magnetite occurs as anhedral crystals throughout the groundmass.

The amygdule minerals are plagioclase, adularia, diopside, magnetite, sphene, chlorite, epidote, calcite, and garnet. In general, chlorite, magnetite, sphene, epidote, diopside, and calcite are found in the centers of the amygdules while the peripheries are coated with the feldspar. Some of the adularia contains radiating needles of an altered silicate which appears to be altered in turn to hematite. Sphene, about 5%, is everywhere found near the opaques and occurs as anhedral masses. Epidote, about 4%, is commonly anhedral to subhedral and typically has striking yellow pleochroism. Chlorite, about 3%,



shows anomalous blue and purple birefringence and occurs as radiating flaky aggregates. Magnetite occurs as anhedral crystals in plagioclase and chlorite. Some of these opaque minerals are altered to hematite and sphene. The feldspar of the amygdules is dusty and altered to sericite; some of it contains albite twinning whereas most of it lacks any twinning except a few Carlsbad twins.

A chemical analysis was obtained for sample N-51 from this flow, and the results are shown in Table 3. Chemically, this flow is classified as an alkali basalt, based on MacDonald and Katsura's (1964) classification.

#### Flow F

Field Observations: This flow forms the uppermost 45 to 50 feet of the hill on which the Cloquet water supply tank is situated. It is traceable to the south along strike where it crops out again in the upper part of the high bluff just north of Highway 61. This location is the same as that of Flow E. It overlies Flow E, and the lower portion of the flow is vesicular and amygdaloidal. No overlying flow could be seen here, but to the south, across Highway 61, the overlying Unit G is present. At this location, the upper portion of Flow F is amygdaloidal with chlorite in the amygdules. From these latter two localities, it appears as though the flow is about 90 feet thick.

Mineralogically, the flow is similar to the basal flow, in that it contains black, blocky augite phenocrysts. It grades upward into a less porphyritic but more ophitic basalt. The weathered surface shows brown, weathered holes suggesting the presence of olivine or an olivine pseudomorph.

Petrography: This flow is very similar to the basal flow, and the reader is referred to the description for Flow A. The only noteworthy difference is that the plagioclase is much fresher in this flow and has a composition of An<sub>48-56</sub>. Since this flow is only about one-third of a mile from the base of the gabbro, the plagioclase may be recrystallized.

A chemical analysis was obtained for sample N-4 from this flow, and the results are shown in Table 3. Chemically, this flow is classified as a tholeiitic basalt, based on MacDonald and Katsura's (1964) classification.

#### Unit G

Field Observations: Unit G is a composite of several flows, the contacts of which cannot be accurately established from field work due to scarcity and discontinuity of exposure. This unit is probably some 500 feet thick and is truncated by the gabbro to the east and north. To the west, the lowermost flow of this unit directly overlies Flow F. The first occurrence of these flows is just to the south of Highway 61 where a large dome-like hill (SW 1/4 of SE 1/4, Sec. 20, T 49 N, R 15 W) shows three distinct flows. Tracing these flows to the south is difficult due to lack of outcrop; however, about 1,500 feet north of Magney Park a few north-south trending outcrops occur and these appear very similar to those seen at the northernmost outcrop.

In the field, the rocks composing this unit are recognized as gray, fine-to medium-grained, massive subophitic or poikilitic basalts. Where contacts between flows occur, the tops are commonly rubbly and always amygdaloidal. Basal portions are somewhat amygdaloidal and

straight pipe vesicles are occasionally present. At one locality, there were straight vesicle cylinders near the bottom of the flow.

Petrography: Thin section study of the flows in Unit G shows that these are either subophitic or poikilitic basalts. The plagioclase is commonly dusty and altered to sericite except nearer the contact with the Duluth Complex where it is fresher.

Plagioclase makes up about 45% to 50% of the rocks, occurs as laths up to 2 mm long, commonly shows albite twinning, and, according to index of refraction studies and the Michel-Levy method, has a composition of  $An_{36-42}$ .

Ophitic subcalcic augite is still present in most of the flows and makes up about 13% to 14% of the rock. However, most of the augite has been altered to actinolite, which makes up about 28% to 31% of the rock. Individual augite crystals are all less than one mm in diameter in subophitic flows but are up to 2 mm in diameter in poikilitic flows (in which the ophitic augite is pseudomorphed by actinolite).

Olivine pseudomorphs, which occur as both phenocrysts and intergranular grains, are present in some of the flows in Unit G. In general, the olivine has been completely replaced by chlorite and/or serpentine which has since been oxidized to a more birefringent type. Magnetite commonly forms rims on the pseudomorphs (see photomicrograph, Figure 8B).

Opagues, mainly ilmenite and magnetite, make up anywhere from 1% to 8% of the rocks; the smaller amounts occur in the contact-metamorphosed zone. Where not affected by the Duluth Complex, the opagues are characteristically altered to sphene and hematite with relict scraps of ilmenite and skeletal magnetite.

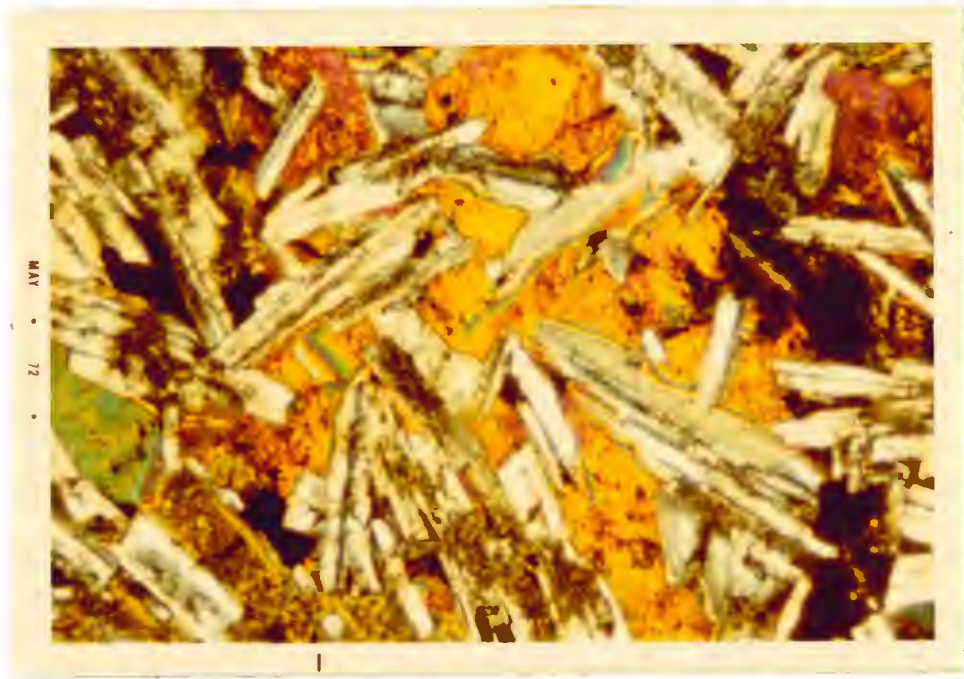
Within about 250 yards of the contact with the Duluth Complex, the rocks of Unit G show a good deal of recrystallization. The most noteworthy change, texturally, is in the disappearance of primary igneous textures and the appearance of a granoblastic texture. Within about 100 yards of the contact, the granofels contains plagioclase, clinopyroxene, and olivine which have been formed by recrystallization of the altered basalt. Within about 100 to 250 yards of the contact with the Duluth Complex, the rock is still granoblastic but biotite, hornblende, and plagioclase are present. Past a distance of about 250 to 300 yards from the contact with the Duluth Complex, the flows show primary igneous textures and minerals such as laths of plagioclase and either pseudomorphs of pyroxene or primary igneous pyroxene and olivine pseudomorphs.

Amygdule minerals include quartz, epidote, prehnite, calcite, chlorite, magnetite, adularia, and sphene in the non-contact metamorphosed basalts. Within 200 yards of the contact with the Duluth Complex, in the contact-metamorphosed basalts, plagioclase occurs as an amygdule mineral.

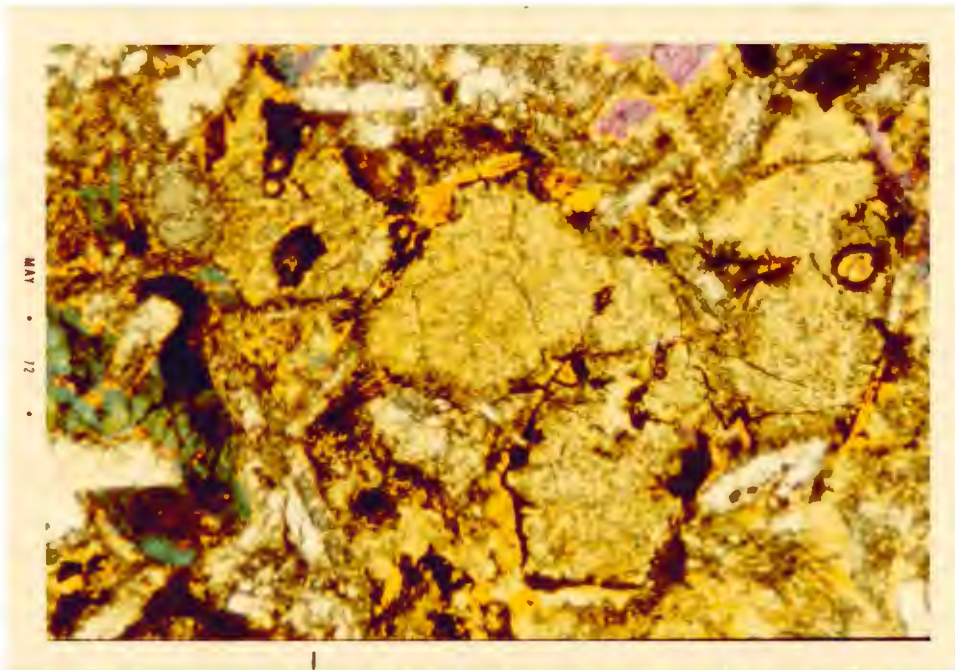
#### Flow H

Field Observations: This flow is best seen in a deep railroad cut near the southernmost extent of the map area west of Gary (NW 1/4, Sec. 4, T 48 N, R 15 W). It is recognizable by its poikilitic texture, as actinolite pseudomorphs after augite yield a patchy appearance when the rock is held in reflected light. The flow is gray and coarse-grained, and has a thickness of 110 to 120 feet. Flow H is underlain by a fine-grained, ophitic basalt which forms the uppermost





A. Photomicrograph of a flow from Unit G showing poikilitic (relict ophitic) texture -- actinolite after augite and plagioclase.



B. Photomicrograph of olivine pseudomorphs rimmed by magnetite, Flow L.

1mm



flow of Unit G. In its upper portions, Flow H is fine-grained and amygdaloidal with chlorite filling the vesicles.

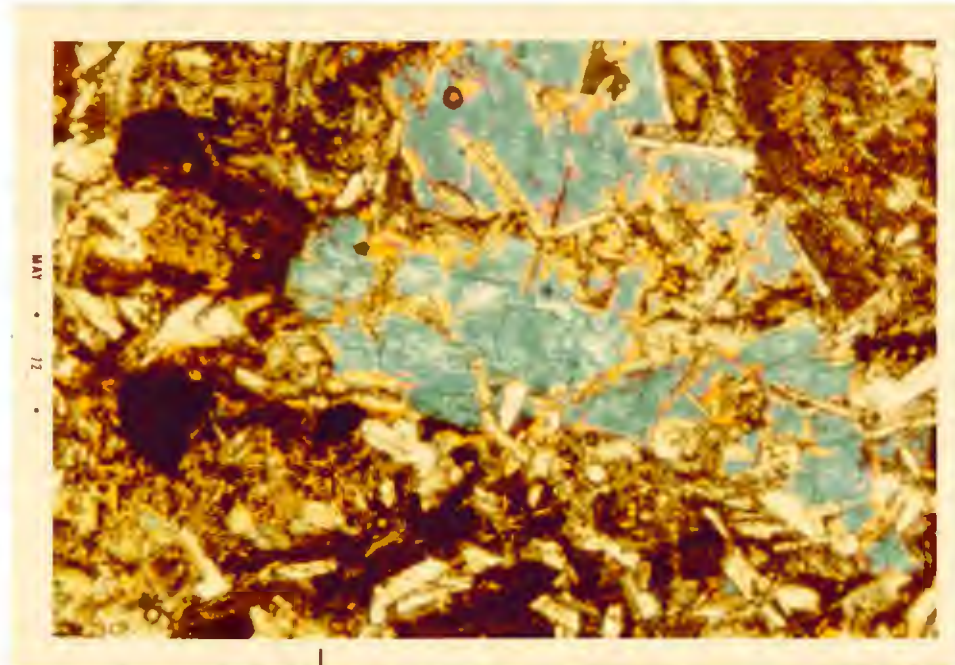
Petrography: Thin section study of this flow shows a poikilitic texture with magnetite and actinolite after augite being the principal ferromagnesian minerals. The actinolite, making up about 30% of the rock, occurs as pseudomorphs of ophitic augite crystals which range in size from 3 to 6 mm in diameter.

Also present in this flow are olivine pseudomorphs. The present mineral appears to be an oxidized serpentine or chlorite showing moderately weak birefringence, up to first order yellow and orange. The size of these crystals is roughly that of the actinolite. No fresh olivine remains, whereas a few relict augite oikocrysts are still present.

Platy ilmenite crystals up to 1.5 mm long are present and show alteration corresponding to the zone I type of Hubbard and others (1970). Magnetite appears as intergranular material less than 1 mm in diameter. It also shows alteration of the zone I type mentioned above. Some of the plagioclase laths, which are up to 2 mm long, are fresh and others are dusty; in many cases they are fresh on the peripheries and dusty in the middle portions. They show either Carlsbad or albite twinning and compositions range from An<sub>38</sub> to An<sub>44</sub>.

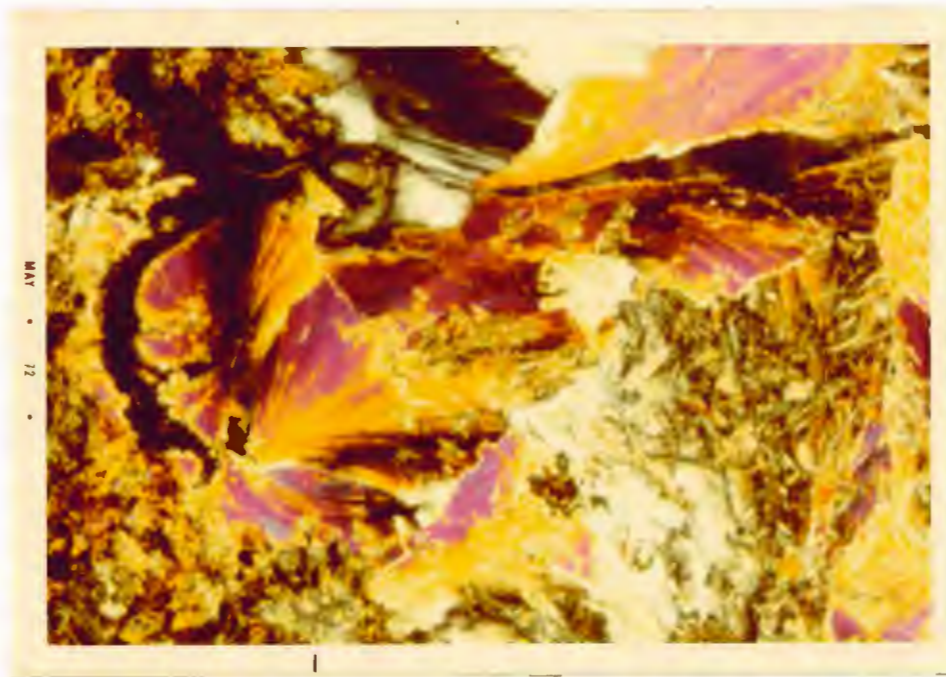
Other minerals present include chlorite and sphene in association with alteration of the ferromagnesian minerals.

A chemical analysis was obtained for sample N-89 from this unit, and the results are shown in Table 3. Chemically, this flow is classified as an alkali basalt, based on MacDonald and Katsura's (1964) classification.



Photomicrograph of a poikilitic basalt showing a large actinolite pseudomorph after augite, from Flow F.

1mm



A. Photomicrograph of prehnite in an amygdule, from Flow I.



B. Photomicrograph of basalt hornfels from within 100 yards of the contact with the Duluth Complex. Olivine, diopsidic augite, and plagioclase make up the rock, from Flow P.

1mm



## Flows I-P

Field Observations: Flows I through P are here combined into one description because they occur in the same area and consist of only two general flow types. It should be noted that Flow I itself is actually a composite of three thin flows or flow units with a total thickness of 30 to 35 feet. The other flows, J through P, are shown in Figure 2 as individual flows.

In general, the flows crop out in the Magney Park area (SW 1/4, Sec. 28 and SE 1/4, Sec. 29, T 49 N, R 15 W) and continue south for about one and one-half miles. Thicknesses range from about 10 feet in Flow I to over 100 feet in the uppermost flow (P).

Petrographically, the flows are either subophitic or ophitic basalts. They are mostly gray to dark gray and either medium or coarse-grained corresponding to flow thickness -- thicker flows are coarser-grained. Toward the base and top of flows, the rock is finer-grained and usually amygdaloidal. In some flows, the tops are rubbly and amygdaloidal, while bottoms are amygdaloidal and in some exposures contain pipe amygdules. Other structures include toes (indicating on-land deposition), billowy and ropy surfaces. Earlier descriptions of the ophitic to subophitic and poikilitic flows in Unit G are also valid for describing the petrography of Flows I through P.

Chemical analyses were obtained for sample N-100 from Flow K and for sample N-124 from Flow O, and the results are shown in Table 3. Chemically, Flows K and O are alkali basalts, according to the classification of MacDonald and Katsura (1964).

## Mafic Dikes

Field Observations: A swarm of mafic dikes intrudes the flows in the southern portion of the map area. These dikes are vertical and follow a N 30° E joint set and can be recognized because they have been preferentially eroded, leaving pronounced trench-like lineaments in the topography. Outcrops of only five dikes were seen in the field; however, other pronounced lineaments running parallel to these dikes constitute strong evidence that at least eight dikes, and possibly more, are actually present in the area. They are part of a swarm that cuts the Thomson Formation for at least six miles to the west (Wright, Mattson, and Thomas, 1970).

The dikes are black, fine-grained basalts which weather to a reddish color. No columnar joints were seen but the dikes have a blocky joint system. Chilled margins are only one or two inches wide, and thicknesses of the dikes vary from about 10 feet to about 50 feet.

Petrography: Thin section study of the mafic dikes reveals that they are subophitic basalts. Plagioclase makes up about 53% of the rock and has a composition of An<sub>33-36</sub>. Some phenocrysts of plagioclase up to 2 mm long are present; however, these total only one percent of the rock. The plagioclase is only slightly dusty and much is partly altered to chlorite.

The primary ferromagnesian minerals appear to be completely replaced by a green pleochroic layer silicate mineral. Birefringence of the mineral (about 300 mu) is too low for biotite and too high for chlorite; and a small 2V and negative sign indicate that the mineral could be biotite, chlorite, or vermiculite. Vermiculite appears to



be the best possibility since its birefringence is weaker than biotite but stronger than chlorite. This mineral makes up some 25% of the rock. Other minerals present include hornblende (3%), and ilmenite and magnetite (8%). Chlorite, sphene, calcite, and epidote make up the remaining 11% with the bulk of this being chlorite and sphene.

### Diabasic Intrusion

Field Observations: Along the hillside west of the Cloquet water supply tank, a diabasic intrusion was found between Flows C and D. No actual contact could be found, but a thickness of about 20 feet is inferred from scattered outcrops. This intrusion could be the surface manifestation of what Mattis (1972) inferred by gravity studies to be a hidden mafic intrusion at depth. Since no contacts were observed between the flows and the diabasic intrusion, it is not known whether the intrusion is a dike or a sill. In outcrop, the rock is brown, medium-to coarse-grained diabase.

Petrography: Thin section study reveals that the rock is ophitic diabase. Minerals include plagioclase, about 50%, with a composition of about An<sub>60</sub>. These plagioclase laths are up to 4 mm long and are included in clinopyroxene crystals which range up to 6 mm in diameter. The plagioclase is fresh and shows albite, pericline, and Carlsbad twinning.

Clinopyroxene makes up about 25% of the rock and commonly shows uranalitization on grain boundaries and along cracks. It occurs in ophitic intergrowth with the labradorite.

Ilmenite and magnetite make up about 10% of the rock and show a good deal of alteration to biotite and hematite. The alteration of the opaques compares to the type I of Hubbard and others (1970). About 3% of quartz is present, which sometimes forms a myrmekitic texture with plagioclase. Chlorite and apatite also occur in minor amounts.

#### Interflow Sediments

Field Observations: A total thickness of about six or eight inches of interflow sediment was found throughout the entire study area. The main occurrence of the sediments is along the hillside just south of Highway 61. Here, two thin interflow units separate Flows E from F and Flows F from G, but neither is continuous along strike. The only other occurrence found is a small, clastic dike, 5 inches thick and nearly vertical, in the Arrowhead Blacktop Quarry (NE 1/4, Sec. 32 and NW 1/4, Sec. 33, T 49 N, R 15 W).

In outcrop, the sedimentary lenses are usually laminated, grayish-brown to black, fine-grained shale to siltstone. In thin section, the grains are angular and moderately sorted. Mineralogically, plagioclase clasts make up about 55%, chlorite about 20%, and quartz about 10% of the rock. Cement is black iron oxide, about 10%, and micas, sphene, and epidote make up about 5%. It appears as though the sediments were derived directly from proximal lava flows.

#### Microgranitic Dikes

Field Observations: Near the southeastern-most portion of the study area, within about 200 yards of the contact with the Duluth Complex,

the flows are intruded by a few granitic dikes which are mostly less than a foot thick.

Petrographically, the dikes are composed of very dusty sericitized plagioclase (25%), very dusty kaolinitized orthoclase (45%), quartz (24%), opaques (4%), and minor amounts of hornblende, actinolite, and chlorite. The actual classification of the rock borders on the granite-quartz monzonite boundary. Grain size is usually on the order of a millimeter or less, although some larger potassium feldspar grains can be seen.

#### Petrographic Description of the Basal Flows on Lucille Island

Six samples collected by J. C. Green from the basal flows on Lucille Island east of Grand Portage, Minnesota (Cook County) were studied in thin section and hand specimen for purposes of correlation with the Ely's Peak basalts. The flows on Lucille Island form part of the basal section of the North Shore Volcanic Group on the northwest limb of the Lake Superior syncline and are a part of Green's (1972) Grand Portage lavas. These flows directly overlie a basal quartz sandstone (Puckwunge Formation) as do the flows in the map area. The following descriptions are offered as evidence that the flows on Lucille Island and the Ely's Peak basalts are petrographically similar and, therefore, may be petrogenetically correlative. That is, they may have been derived from the same parent magma under the same conditions of magma generation.

Petrography: The flows described herein are massive, dark green, fine-grained augite-porphyrific basalt. According to Green (1972), this

type of flow makes up the basal 250 feet of the section on Lucille and Magnet Islands. Six thin sections were studied. Single and glomeroporphyritic augite phenocrysts up to 3 mm in diameter make up 30% of one sample and 46% of the other. The phenocrysts are euhedral to subhedral, some are zoned, and some show twinning on the (100) twin plane. Some of the augite is altered to pale green, pleochroic actinolite and chlorite on crystal edges, along cracks and cleavage traces. The more porphyritic sample is PP-16, for which a chemical analysis is given in Table 3 and composition plotted in Figures 4A and B.

Plagioclase makes up about 22% of the more porphyritic basalt and 34% of the less porphyritic sample. It is dusty in the less porphyritic rock, altered to sericite, and occurs as laths up to 1 mm long. In the more porphyritic rock the plagioclase is fresh, up to 1 mm long, and has a composition of  $An_{43-47}$ .

In the more porphyritic sample, pseudomorphs after olivine phenocrysts make up about 15% of the rock. They are composed of chlorite or serpentine which has been oxidized to a more birefringent type and are about 1 to 2 mm in diameter. In the other sample, olivine pseudomorphs make up about 2.5% of the rock and are mineralogically identical to those of the more porphyritic rock. Ilmenite and anomalous-purple birefringent chlorite are also seen in the pseudomorphs of olivine.

Ilmenite blades up to 2 mm long make up about 7% of the less porphyritic sample and about 4% of the more porphyritic rock. In both rocks, the magnetite makes up a very small percentage and occurs as small, blocky crystals in the groundmass. The opaques in both rocks are altered, with sphene and hematite as alteration products. The



alteration appears to correspond to the type I of Hubbard and others (1970).

The less porphyritic rock also contains possible altered glass, calcite, sphene, quartz, and epidote as interstitial material.

### Correlation

The augite-porphyrific flows that make up the basal portion of the Ely's Peak basalts and the augite-porphyrific rocks from the basal flows on Lucille Island, near Grand Portage, Minnesota, are petrographically very similar, as can be seen from the above flow descriptions. Chemically, the flows in these two areas are also very similar, and this, together with the geologic occurrence of these flows, also suggests correlation (in each area, the flows are situated at the base of the volcanic pile).

Geophysical studies on the magnetic polarity of the flows at the two locations have been reported by Green and Books (1972). Based on their findings, the flows at Grand Portage, Minnesota and the Ely's Peak basalts are both magnetically reversed, which indicates that both of these groups of flows were deposited during the same paleomagnetic interval, that interval corresponding to Lower Keweenawan time.

Based on the paleomagnetic data, it can be concluded that the flows in the two areas show a general, broad time equivalence. In addition, the petrographic and chemical data show remarkable similarity of the flows in the two areas. From this, it can be seen that the flows from the two areas had a similar mode of origin and source; and a structural and sequential similarity show a similar tectonic-historical-stratigraphic situation at the time of extrusion of these flows.



A-F-M-DIAGRAM

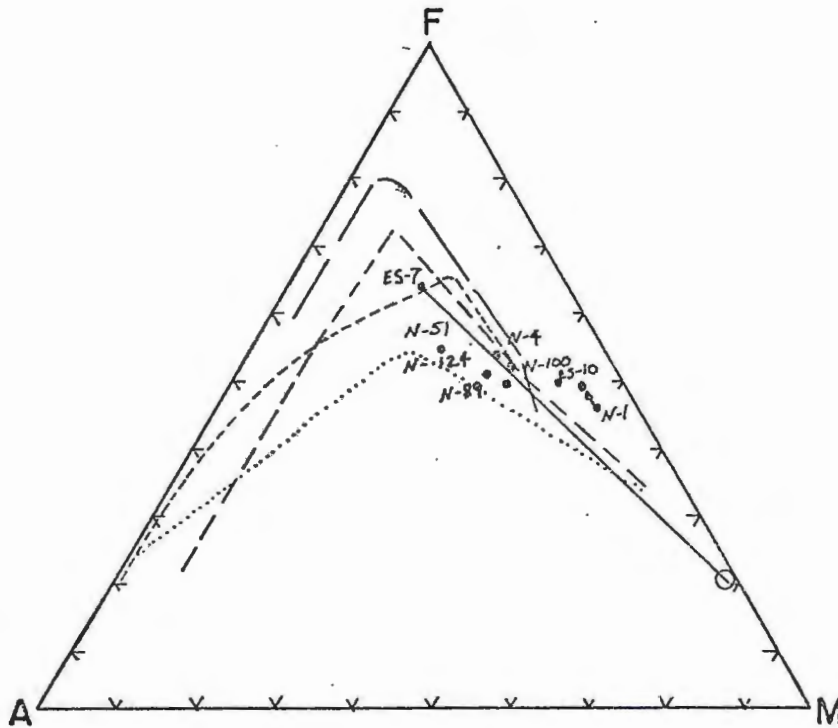


Figure 11: A-F-M diagram (A=Al<sub>2</sub>O<sub>3</sub>, F=Total Iron, M=MgO) showing differentiation trends in the Skaergaard Intrusion (long dashes), Hawaiian tholeiites (medium dashes), Hawaiian alkali basalts (dots), Thingmuli volcano, Iceland (short dashes), and Ely's Peak basalts (solid line). Also plotted on the diagram is the average composition of augite phenocrysts in the Ely's Peak basalts (open circle).

## VARIATION DIAGRAMS

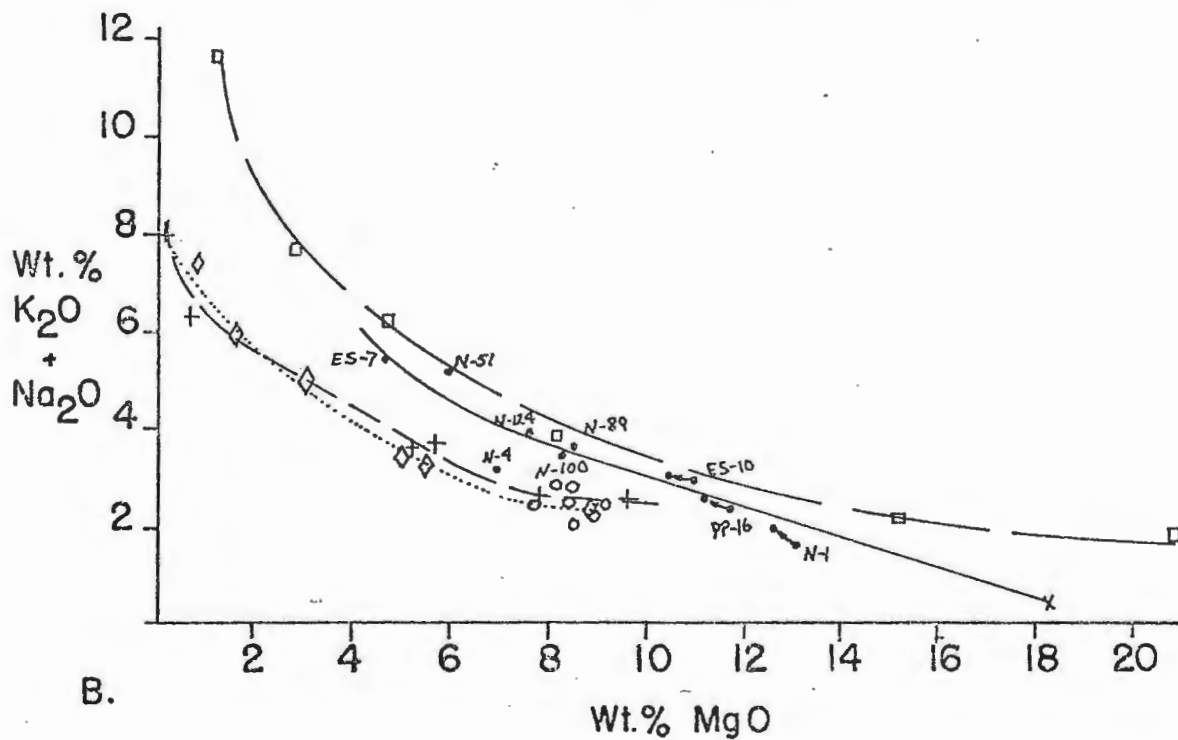
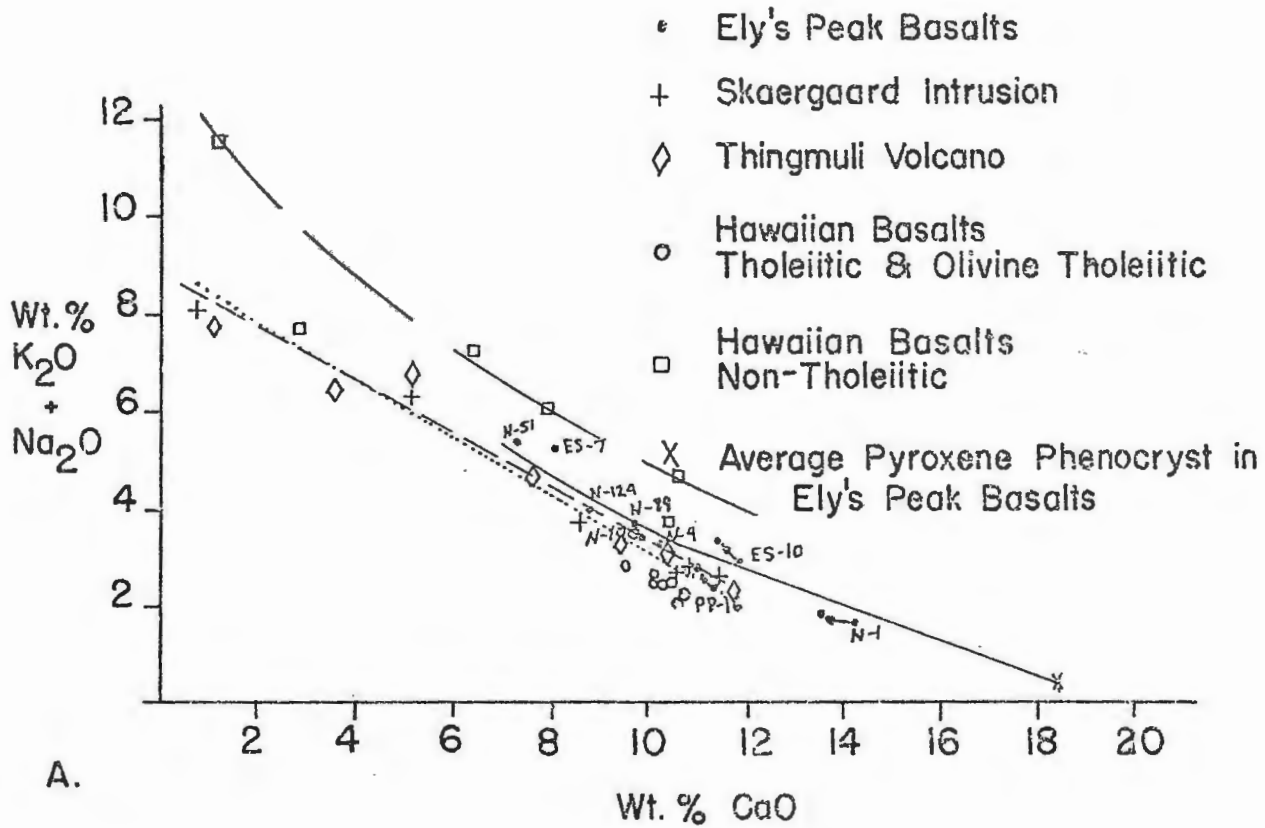


Figure 12

### Variation Diagrams and Differentiation Trends

In Figure 11, the differentiation trend of the Ely's Peak basalts is shown on an alkali-iron enrichment diagram and is compared with trends of the Skaergaard Intrusion (Wager, 1960), the tholeiitic and alkalic trends of Hawaii (MacDonald and Katsura, 1964), and the Thingmuli Volcano of Iceland (Carmichael, 1964). As can be seen on the diagram, the general trend is the same for the Skaergaard, Thingmuli, Hawaiian tholeiites and Hawaiian alkali basalts, though the latter show much less iron enrichment. Since no intermediate to felsic flows are present in the Ely's Peak basalts, it is not known whether the same trend exists for this group. However, the plot does show that there is a general enrichment in iron and total alkalis and a depletion of magnesia. The average chemical analysis of the augite phenocrysts is also plotted on the diagram and falls near the magnesia corner. Since two of the flows (represented by N-1 and ES-10) are augite-porphyrific, and since the average composition of the phenocrysts from these flows are plotted on the diagram, a trend line can be drawn between the average phenocryst composition and the points representing the composition of the flows.

In Figure 12A, lime is plotted against total alkalis; and in Figure 12B, magnesia is plotted against total alkalis. The trends of the Ely's Peak basalts are plotted, as are the trends of the Skaergaard Intrusion, Thingmuli Volcano, Hawaiian tholeiites and Hawaiian alkali basalts. Inspection of the diagrams shows similar trends of lime and magnesia impoverishment with increase in total alkalis for all the groups plotted. The Hawaiian tholeiites do not have a well-developed trend since they have a limited range of CaO and MgO content.

Comparison of the Ely's Peak basalts with the Skaergaard Intrusion and the Thingmuli Volcano shows that the Ely's Peak basalts are slightly richer in alkalis but poorer in total alkalis than the Hawaiian alkali basalts.

The average chemical analysis of the pyroxene phenocrysts of the Ely's Peak basalts is also plotted in Figures 12A and 12B. As before, the compositions of these augite-porphyrific flows are connected to the composition of the flows in which the phenocrysts occur by a trend line. From these diagrams, it can be seen that there is a trend from lime and magnesia-rich to alkali-rich basalts for the Ely's Peak flows.

Based on the compositions of the pyroxene phenocrysts in the porphyritic flows, it is thought that they crystallized early and at a shallow depth. Chemical evidence for this hypothesis is the high Mg and Ca content of the phenocrysts, the low Fe (possibly indicating high temperature), and the low alumina content (possibly indicating low pressures and, therefore, shallow depth).

From the earlier subtraction calculations, the readjusted compositions are plotted on the variation diagrams in Figures 12A and 12B for samples N-1 and ES-10. From this, it can be seen that the bulk composition of the original melt prior to pyroxene phenocryst crystallization may have been alkalic. Therefore, by augite fractionation, the composition of the residual liquid may have changed to a more tholeiitic melt.

#### Crystallization History

The crystallization history of the Ely's Peak basalts can be inferred from textural and mineralogical relations within the flows.



Based on structures within the flows, such as ropy surfaces, pipe vesicles, and crystal settling, it can be inferred that nearly all of the lavas probably had low viscosity. From the grain size of the flows and general lack of crystal orientation, it appears likely that crystallization in most flows occurred after flowage had ceased. Thus, the development of some medium-to coarse-grained flows was permitted by static crystallization. A generalized crystallization history of the two main flow types (porphyritic flows and ophitic and subophitic flows) will now be presented.

Pyroxene-Porphyritic Flows: The pyroxene-porphyritic basalts show clear evidence of two periods of crystallization. The first period of crystallization was prior to extrusion of the flows when pyroxene crystallized early at high temperatures and shallow depths. After extrusion of the flows and subsequent cessation of flowage, the lava was apparently viscous enough to allow some settling of the pyroxene phenocrysts. The second period of crystallization was marked by simultaneous crystallization of plagioclase, clinopyroxene, and probably ilmenite to form a subophitic groundmass.

Non-Porphyritic Flows: The non-porphyritic flows include ophitic and subophitic basalts, some of which contain pseudomorphs of olivine. In these flows, it can be inferred that olivine crystallized early (probably shortly after flowage ceased) and was quickly followed by simultaneous crystallization of plagioclase and clinopyroxene. In flows where ilmenite and magnetite occur as small phenocrysts, they probably crystallized early; but more often they occur as intergranular material indicating late crystallization and, therefore, iron-enrichment of the residual fluid.

### Parent Magma

The Ely's Peak basalts have been classified as either tholeiitic or alkalic basalts according to the classification scheme of MacDonald and Katsura (1964) (see Table 5). If this comparison is valid, then by using Green, Green, and Ringwood's (1967) experimental results on the origin of basaltic magma, it should be possible to deduce something about the magma from which the Ely's Peak basalts were derived.

According to the model of Green, Green, and Ringwood (1967), basaltic parent magma is derived by partial melting from a pyrolite mantle. The alkali basalts originate from magma segregation or fractional crystallization processes at depths of 35 to 60 km. If a fairly large degree of partial melting of pyrolite takes place, the magma segregation at these depths would yield an olivine tholeiite magma. If a smaller degree of partial melting takes place at these depths, the resulting magma is alkali basalt. Both of these magmas could undergo fractional crystallization upon rising to produce different lava types.

For comparison of flow types in other well-studied areas and the Ely's Peak basalts, Table 9 presents chemical analyses of Hawaiian tholeiites, Thingmuli Volcano quartz tholeiites, lunar KREEP samples, and different flow types of the Ely's Peak basalts. From these analyses, it can be seen that the alkali basalts and the augite-porphyrific basalts of the Ely's Peak flows are chemically similar to the Hawaiian tholeiites; and also, the quartz tholeiites of the Ely's Peak basalts are chemically similar to the Thingmuli Volcano quartz tholeiites. It can be seen from the analyses on this table that each flow type has its own chemical affinities that reflect the physical conditions of magma generation. For

example, quartz tholeiite basalts, according to Green, Green, and Ringwood (1967), undergo magma segregation at depths of 15 km or less. They indicate that quartz tholeiites could also form by fractional crystallization of a high-alumina basalt magma, alkali basalt magma, or olivine tholeiite magma at depths of 0 to 15 km.

|                                | (1)         | (2)         | (3)         | (4)         | (5)         | (6)        |
|--------------------------------|-------------|-------------|-------------|-------------|-------------|------------|
| SiO <sub>2</sub>               | 49.36       | 50.20       | 48.13       | 50.45       | 46.71       | 48.2       |
| TiO <sub>2</sub>               | 2.50        | 3.19        | 1.48        | 1.13        | 2.37        | 1.9        |
| Al <sub>2</sub> O <sub>3</sub> | 13.94       | 12.90       | 9.96        | 13.58       | 13.68       | 15.5       |
| Fe <sub>2</sub> O <sub>3</sub> | 3.03        | 3.31        | 1.53        | 3.54        | 3.73        | ---        |
| FeO                            | 8.53        | 11.88       | 11.10       | 10.13       | 10.23       | 10.7       |
| MnO                            | 0.16        | 0.27        | 0.15        | 0.19        | 0.18        | ---        |
| MgO                            | 8.44        | 4.78        | 10.55       | 6.94        | 6.82        | 7.8        |
| CaO                            | 10.30       | 9.27        | 11.57       | 10.13       | 8.65        | 10.9       |
| Na <sub>2</sub> O              | 2.13        | 3.07        | 2.00        | 2.41        | 3.25        | 0.45       |
| K <sub>2</sub> O               | 0.38        | 0.57        | 0.78        | 0.71        | 1.12        | 1.2        |
| P <sub>2</sub> O <sub>5</sub>  | <u>0.26</u> | <u>0.58</u> | <u>0.22</u> | <u>0.25</u> | <u>0.37</u> | <u>0.7</u> |
| TOTAL                          | 99.03       | 100.01      | 99.98       | 99.47       | 99.80       | 97.35      |

- (1) Average of 181 Hawaiian tholeiites (MacDonald and Katsura, 1964, p. 124)
- (2) Average of 7 (quartz) tholeiites, Thingmuli Volcano (Carmichael, 1964, p. 439)
- (3) Average of 3 augite-porphyrific tholeiites from Ely's Peak basalts
- (4) N-4, quartz tholeiite from Ely's Peak basalts
- (5) Average of 4 alkali basalts from Ely's Peak basalts
- (6) Average of 22 fragments of KREEP glass (Hubbard et al., p. 343)

Table 9

Based on the chemical nature of the flows, that is, alkali basalts, it is thought that the Ely's Peak basalts were derived by a small degree of partial melting of pyrolite at depths of 35 to 60 km. It is possible, though, that fractionation of this "original" parent magma took place, upon rising, to produce flows with different chemical and mineralogical characteristics such as olivine tholeiite and quartz tholeiite basalts, which are flow types present in the Ely's Peak basalts.

The actual flow types that could represent the parent magma are the non-porphyrific alkali basalts such as N-89 from Unit G and N-100 from Flow K. On the variation diagrams of Figure 12, it can be seen that when the compositions of these two basalts are plotted, they fall close to each other. In addition, when subtraction calculations are done of the excess pyroxene phenocrysts, the augite-porphyrific tholeiite flow types (N-1 from Flow C and ES-10 from Flow A) plot near the same area as the alkali basalts because the readjusted chemical analyses bear close resemblance to alkali basalts and may represent the composition of the original magma.

Other chemical characteristics of the Ely's Peak basalts are slight enrichment of  $P_2O_5$  and  $K_2O$  which compare to the "KREEP" rocks brought back from lunar expeditions (see Table 9). The word "KREEP" denotes rocks which Hubbard and others (1970) found to be rich in potassium, rare earth elements, and phosphorous. Average  $K_2O$  content in the lunar "KREEP" samples is about 1.2%, and average  $P_2O_5$  content was found to be about 0.7%. (For rare earth element analyses, see Hubbard and others, 1970).

Although no rare earth studies have been done on the Ely's Peak basalts, they could conceivably contain significant amounts of rare earth elements similar to the amounts in the "KREEP" samples. Hubbard and others (1970) suggest that the "KREEP" rocks originated by extreme differentiation of an igneous liquid or a liquid produced by very small degrees of partial melting. This theory is consistent with the idea that the alkali basalts formed by small degrees of partial melting as put forth earlier for the origin of the parent magma that produced the Ely's Peak basalts.



## Discussion

The North Shore Volcanic Group has been referred to by White (1960) as flood basalts. Since the Ely's Peak basalts form the basal part of the North Shore Volcanic Group, they are included in this classification as flood basalts. Although the flows appear to have been extruded in sheet-like masses, one on top of the other, care must be exercised in labeling them as flood basalts. This is simply because not enough exposure exists so that they can be traced for long distances, and, typically, flood basalts are characterized by their wide areal extent. The area encompassing the Ely's Peak basalts (about 8 miles by 1 mile) could hardly be called a large geographic area, and thus, the actual development of large sheets of basalts cannot be substantiated. The farthest distance an individual flow could be traced in this area was about three miles; but the limits are imposed by the lack of exposures, not by demonstrable endings of individual flows. These flows may be flood basalts; but in the writer's opinion, they cannot be positively classified as such on the basis of field observations alone.

If a chemical comparison is made to other areas where known flood basalts occur, then classification as flood basalts may be partially based on chemical characteristics. In general, the Ely's Peak basalts do not bear close resemblance to the basalts of the Columbia Plateau or the Deccan Plateau (which are known to be flood basalts) because of higher silica content in the latter two (see chemical analysis, Table 10). The Ely's Peak basalts bear a close chemical resemblance to the flood basalts in Iceland (see Table 10) and on this criterion the Ely's Peak basalts may be classified as flood basalts chemically similar to the Iceland flood basalts.

|                                | (1)   | (2)  | (3)    | (4)   |
|--------------------------------|-------|------|--------|-------|
| SiO <sub>2</sub>               | 48.75 | 53.8 | 50.61  | 47.71 |
| Al <sub>2</sub> O <sub>3</sub> | 12.12 | 13.9 | 13.58  | 12.14 |
| Fe <sub>2</sub> O <sub>3</sub> | 4.64  | 2.6  | 3.19   | 2.88  |
| FeO                            | 9.61  | 9.2  | 9.92   | 10.32 |
| MnO                            | 0.24  | 0.2  | 0.16   | 0.18  |
| MgO                            | 5.46  | 4.1  | 5.46   | 8.24  |
| CaO                            | 9.71  | 7.9  | 9.45   | 9.93  |
| TiO <sub>2</sub>               | 2.85  | 2.0  | 1.91   | 1.88  |
| Na <sub>2</sub> O              | 2.95  | 3.0  | 2.60   | 2.68  |
| K <sub>2</sub> O               | 0.49  | 1.5  | 0.72   | 0.94  |
| P <sub>2</sub> O <sub>5</sub>  | 0.48  | 0.4  | 0.39   | ---   |
| H <sub>2</sub> O               | 0.82  | 1.2  | 2.13   | ---   |
| CO <sub>2</sub>                | 0.23  | ---  | ---    | ---   |
| TOTAL                          | 99.45 | 99.8 | 100.12 | 96.90 |

- (1) Average chemical analyses of 10 olivine-tholeiite and tholeiite lavas from Thingmuli Volcano, Iceland (Carmichael, 1964)
- (2) Average chemical analyses of 5 Yakima basalts from the Tieton River and Rattlesnake Creek areas, Washington (Swanson, 1967)
- (3) Average of 11 Deccan basalts (Turner and Verhoogen, 1960, p. 208)
- (4) Average of 8 Ely's Peak basalts

Table 10

## METAMORPHIC PETROLOGY

### Introduction

The basal flows forming the Ely's Peak basalts have undergone at least one and possibly two types of metamorphism -- contact metamorphism of the albite-epidote hornfels facies, hornblende hornfels facies, and pyroxene hornfels facies or regional burial metamorphism of the greenschist facies. The metamorphism of the flows is most apparent within about 300 yards of the contact with the gabbro. At distances greater than about 300 yards from the contact, the flows retain their primary igneous textures; and it is more difficult to determine the type of metamorphism (contact vs. regional).

The contact metamorphism was caused by intrusion of the adjacent Duluth Complex. In this type of metamorphism, the basalts are partly or completely recrystallized, and a granoblastic texture is imparted to the rock which is marked by the disappearance of primary igneous textures. However, most primary igneous structures such as amygdules, flow contact, and pipe vesicles are still preserved in the hornfels.

The regional metamorphism is thought to have been produced by rising pressures and temperatures resulting from the deposition of overlying flows and perhaps sediments. This alteration is a hydrothermal type of regional metamorphism and no metamorphic foliation was developed in the flows. In most of the rocks, primary igneous structures and textures are still preserved.

Since the minerals which make up the greenschist facies and the albite-epidote hornfels facies (outermost zone of contact metamorphism)

are the same, and since the Ely's Peak basalts are in contact along one side with the Duluth Complex, the flows may only have been contact metamorphosed. It is believed, however, that the flows were metamorphosed by burial as well as metamorphosed by the Duluth Complex, because flows in Ironwood, Michigan, and at Grand Portage, in northeastern Minnesota, which are petrographically similar to the Ely's Peak basalts, have undergone metamorphism on a regional scale to the greenschist facies (Green, 1972, personal communication). No large igneous intrusion occurs in proximity to the flows in these other two areas. In addition to these two localities, the flows at Leif Ericson Park immediately above the Ely's Peak basalts and the gabbro in the City of Duluth are also metamorphosed to the greenschist to zeolite facies, and the entire overlying part of the North Shore Volcanic Group has undergone zeolitic alteration. By analogy, then, with the flows at these three locations, it is thought that the Ely's Peak basalts also underwent a pervasive hydrothermal, regional metamorphism which, considering the lack of folding, could be called burial metamorphism.

What follows is a description of the metamorphism beginning with the innermost zone of high-grade contact metamorphism and concluding with a detailed description of the outermost, low-grade contact or burial metamorphosed zone.

#### Innermost Contact Zone

The innermost zone of contact metamorphism is about 100 yards wide and is made up of basalt which has been metamorphosed to a granofels of the pyroxene-hornfels facies. For the most part, three minerals make



up the rocks of the innermost zone. These are calcic plagioclase, clinopyroxene, and olivine. Temperatures at the contact can be inferred from the nature of the intrusive rock. The temperature of the magma itself was probably about 1100° C. This produced temperatures of about 600° C to 700° C which metamorphosed the basalts in the innermost zone. These metamorphic temperatures are based on general temperature conditions set forth by Turner (1968) for the pyroxene-hornfels facies.

#### Middle Contact Zone

The middle zone of contact metamorphism is about 150 to 200 yards wide. The innermost zone grades imperceptibly into the middle zone which is marked by the appearance of biotite and minor hornblende with the disappearance of olivine and clinopyroxene. In this zone, the plagioclase is fresh and completely recrystallized. Near the innermost zone, the plagioclase is granular but toward the outermost zone it retains its primary lathy appearance. Temperatures of metamorphism are estimated to have been from about 400° C to 600° C. These are based on general temperature conditions set forth by Turner (1968) for the hornblende-hornfels facies.

#### Outermost Zone

The outermost zone is the widest zone and encompasses all of the flows outside the zone of hornblende-hornfels metamorphism. The middle contact zone grades imperceptibly into the outer zone. The flows in the outer zone have been either contact metamorphosed to the albite-

epidote-hornfels facies, or hydrothermally metamorphosed to the greenschist facies, or both. Textural and mineralogical evidence of regional hydrothermal or contact metamorphism in the Ely's Peak basalts will now be presented in order to establish a basis for estimating the physical conditions of the low-grade metamorphism.

For the most part, the flows retain their original igneous textures up to about 250 to 300 yards from the contact with the Duluth Complex; but, as mentioned above, in the area between this general limit and the contact (herein called the contact zone), the flows are recrystallized to a fine-grained, granoblastic granofels completely lacking any original igneous textures. This latter texture can be used as evidence for contact metamorphism; however, no real textural evidence is present (e.g. foliation or recrystallization) to indicate whether the flows outside of the contact zone have been regionally or contact metamorphosed.

Mineralogically, the flows show an approach to greenschist facies or albite-epidote-hornfels facies because the primary igneous minerals in the flows outside the contact zone are altered to minerals typical of these two facies. Many of the rocks in the outer zone contain relict minerals or grains that show incomplete reaction. It is assumed that the alteration of the minerals in this zone reflect the physical conditions to which the rocks were exposed and to which they were adjusting. Plagioclase often appears dusty, and exhibits a range in composition from calcic oligoclase to sodic andesine. Olivine alteration is complete with only pseudomorphs remaining. These pseudomorphs are composed of chlorite and/or serpentine which is often oxidized to an unusually birefringent type. In general, the clinopyroxene has been altered to actinolite. The phenocrysts of clinopyroxene show the least

alteration, usually only altering along grain boundaries, cracks, cleavage traces, and to some extent along concentric zones of lamellae within the crystals. Intergranular and poikilitic grains of clinopyroxene show a greater degree of replacement by actinolite and are in many cases completely replaced. Opaque minerals, usually magnetite and ilmenite, were also hydrothermally altered. Skeletal magnetite and ilmenite are commonly altered to sphene and hematite. The alteration of the opaques seems to correspond to the type I established by Hubbard, Palmer, and Ade-Hall (1971). This implies hydrothermal alteration at temperatures of about 300° C.

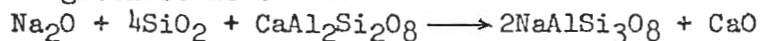
Thus, the mineral assemblage produced in the basalt by hydrothermal alteration or contact metamorphism is:

Sodic Plagioclase + Actinolite + Chlorite + Sphene + Hematite

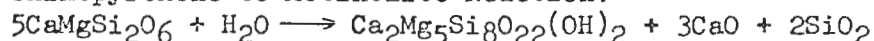
It is quite possible that this assemblage was produced by metamorphism by hydrothermal solutions. The source of these solutions is highly speculative, but the writer concurs with White (1957), who suggests that the rubbly flow tops could have acted as a partial trap for water. Also, since the basal flow is pillowed, it is thought to have been deposited in water. This could, therefore, be another source of the hydrothermal solutions which formed when the lavas were buried by overlying flows.

The following are some general, idealized reactions which may have taken place during metamorphism to transform the primary igneous minerals into the observed mineral assemblage:

Plagioclase Reaction:



Clinopyroxene to Actinolite Reaction:



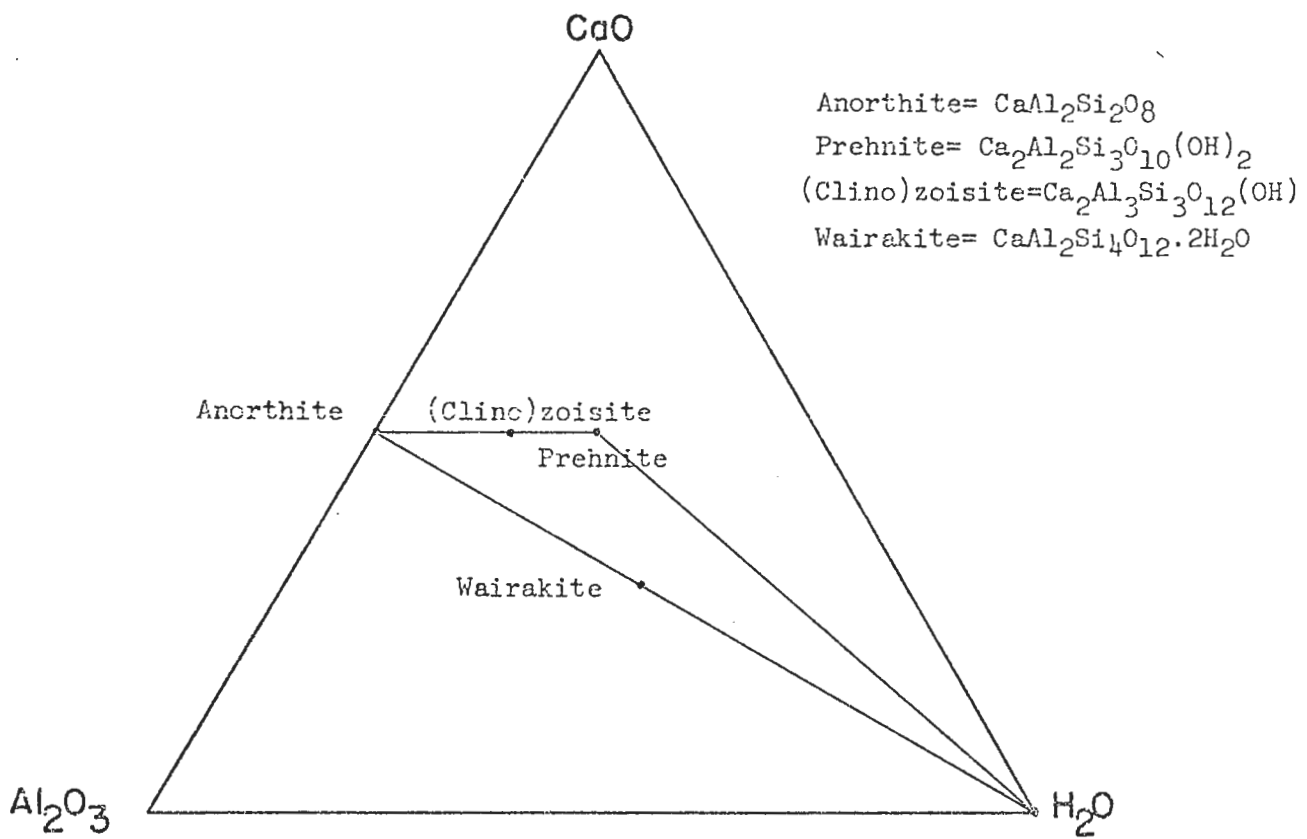
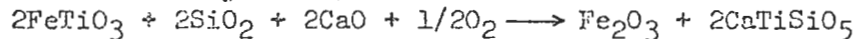


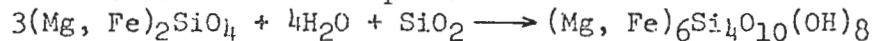
Figure 13. CaO-Al<sub>2</sub>O<sub>3</sub>-H<sub>2</sub>O plot of the common calcium aluminum silicates that occur in the Ely's Peak Basalts.



Ilmenite to Sphene + Hematite Reaction:



Olivine to Chlorite-Serpentine Reaction:



It should be emphasized that these reactions are very ideal, and it has been observed that all but one (olivine to chlorite-serpentine) represent reactions which have not gone to completion because it is common to find unaltered, primary pyroxene, opaques, and unalbitized plagioclase in the Ely's Peak basalts. Thus, there is a possibility that disequilibrium assemblages were produced which are typical of the albite-epidote hornfels facies and possibly the greenschist facies (Turner, 1968).

Other mineral assemblages which may be characteristic of low-grade contact or regional metamorphism are observed in amygdules and veins within the flows. These assemblages are:

Vein Assemblages

Calcite + Wairakite  
Prehnite + Quartz + Calcite + Epidote  
Wairakite + Quartz + Epidote  
Adularia + Calcite + Quartz

Amygdule Assemblages

Epidote + Calcite + Sphene + Chlorite + Plagioclase +  
Magnetite + Diopside  
Calcite + Epidote + Chlorite + Adularia + Actinolite  
Quartz + Actinolite + Epidote + Sphene + Plagioclase  
Calcite + Epidote + Actinolite + Quartz + Chlorite  
Prehnite + Epidote + Quartz + Actinolite  
Plagioclase + Hornblende

It should be noted that these mineral assemblages do not show any type of zonation with distance from the contact with the Duluth Gabbro, except that the more hydrous phases do not exist within 250 to 300 yards of the contact with the gabbro. In general, for amygdule mineral assemblages the calcium-rich phases, e.g. plagioclase, epidote, and prehnite are found on the peripheries of the amygdules whereas the ferromagnesian

mineral chlorite is most common further in toward the centers. In veins, the calcite and prehnite are often on the peripheries with epidote, wairakite, and chlorite occurring further in from these phases.

By considering only quartz bearing assemblages in the system  $\text{CaO}$ ,  $\text{Al}_2\text{O}_3$ ,  $\text{SiO}_2$ ,  $\text{H}_2\text{O}$ , and  $\text{CO}_2$  the chemographic relations can be plotted on a triangular diagram of  $\text{CaO} - \text{Al}_2\text{O}_3 - \text{H}_2\text{O}$  as in Figure 13 to determine if they might be compatible. It should be noted that  $\text{SiO}_2$  and  $\text{CO}_2$  are considered mobile components to be added to or subtracted from the system. From this plot, it appears as though the observed mineral assemblages are compatible, and, therefore, the differences in these assemblages can be simply explained in terms of bulk-compositional differences. It should also be considered what would happen to the compatibility in this system if an additional phase were added to the system. Upon addition of a new phase, an additional component would be needed to describe the phase, and, therefore, according to the phase rule, compatibility between these phases would be maintained.

By considering the possible reactions between the five phases plotted on Figure 13 for quartz-bearing assemblages, a petrogenetic grid can be developed as seen in Figure 14. It should be noted that the slopes of the univariant lines on the grid and the  $300^\circ \text{C}$  and 2,000 bars shown on the figure will be discussed later. When the observed vein and amygdule assemblages are plotted on the grid, all the assemblages could fall compatibly into field I or V on the grid. Thus, all of the mineral assemblages fall onto the low-temperature side of the wairakite-water line. In particular, it might be reasoned that since prehnite and wairakite do not occur together in any of the assemblages, that all of the mineral assemblages could fall into stability field V

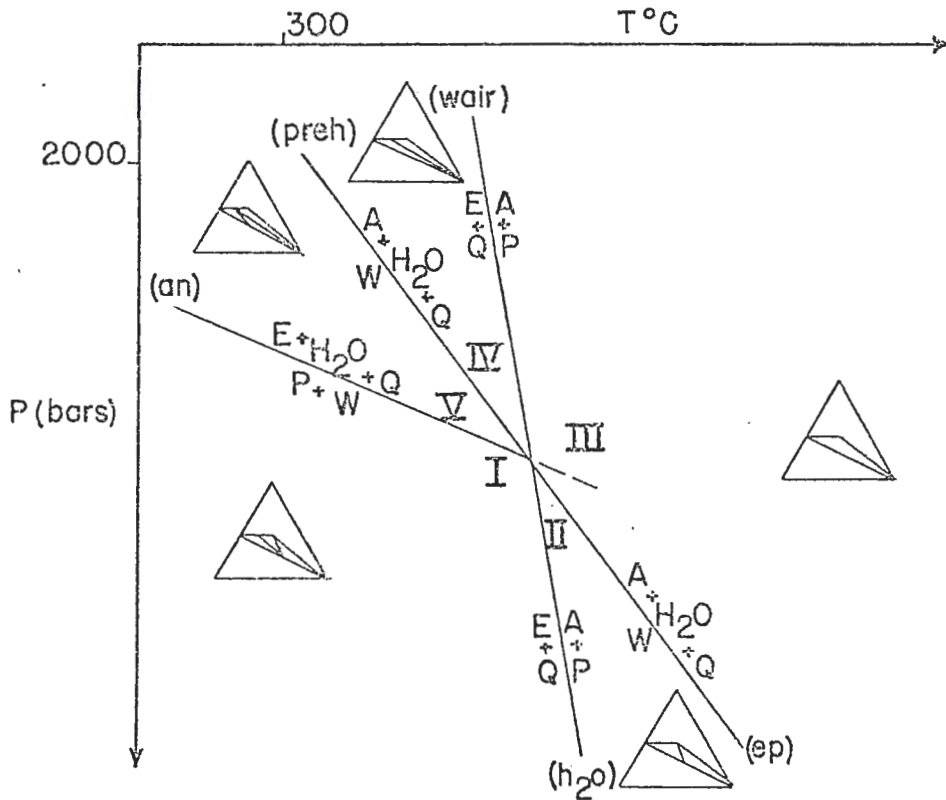
Reactions:

(H<sub>2</sub>O, Wair) Epidote + Quartz = Anorthite + Prehnite

(An) Prehnite + Wairakite = Epidote + H<sub>2</sub>O + Quartz

(Ep, Preh) Wairakite = Anorthite + H<sub>2</sub>O + Quartz

Figure 14



on the grid rather than field I. This field, then, could be one where all the observed mineral assemblages are stable, and therefore, could represent the effective physical conditions. It should also be noted that two types of reactions could occur between minerals in this field, those involving water, and those in which H<sub>2</sub>O is neither a product nor a reactant.

Since two of the commonly observed assemblages (Wairakite + Quartz + Epidote, and Prehnite + Quartz + Epidote + Actinolite) have reactions on the grid that involve decomposition of wairakite to anorthite, quartz and water; and decomposition of anorthite and prehnite to epidote and

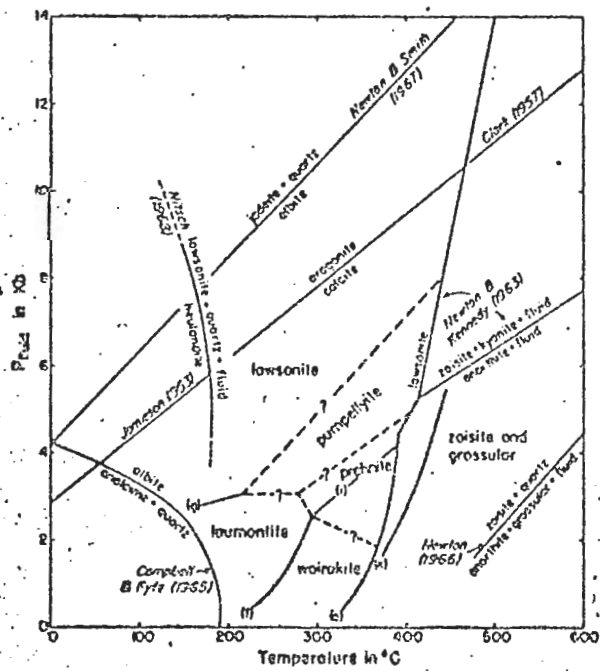


Figure 15: P-T Diagram for numerous critical reactions in low-grade metamorphic rocks illustrating the possible stability field of wairakite and related minerals. From Liou (1970, p. 276).



quartz, attention should now be turned to experimental studies on wairakite and epidote in order to establish a basis for calibrating the grid for temperature and pressure. Liou (1970), states that wairakite forms under two types of conditions; (1) a high-temperature environment resulting from temperature increase due to both burial and local epizonal intrusion of magma, and (2) in active geothermal areas with steep geothermal gradients. From field observations, it appears as though the former of these two environments applies to the Ely's Peak basalts, i.e. burial, and local epizonal intrusion of the Duluth Complex. Other reported occurrences of wairakite attributed to burial and intrusion are in the Pacific Northwest by Wise (1959); by Fiske in Washington (1963); by Whetten in the Virgin Islands (1965); and by Seki in Japan (1966). Optical properties and x-ray data for the wairakite from the Ely's Peak basalts are presented in Appendix A.

From Liou's (1970-71) experimental work on zeolites and related calcium-aluminum silicates certain phase relations denoting specific pressure-temperature conditions have been worked out. Figure 15 shows his  $P_{H_2O}$ - $T$  diagram for numerous critical reactions in low-grade metamorphic rocks illustrating the possible stability field of wairakite and related minerals (Liou, 1970). From the data on Figure 15, it is apparent that the upper stability limit of wairakite is about 2 to 2.5 kilobars pressure and 290° C to 370° C. These, then, probably represent the maximum pressures and temperatures at which wairakite is stable; at higher temperatures and pressures wairakite would break down to form anorthite, quartz, and water, or zoisite, grossular, and water. These values of temperature and pressure may now be used to help calibrate the grid.

It is apparent that no experimental studies have been done involving epidote and quartz going to prehnite and anorthite. Therefore, the temperatures and pressures at which this reaction will take place are not known and cannot be used to calibrate the grid.

It should be noted that the position of the invariant point on the grid (Figure 14) and the slopes of the univariant lines cannot be calculated because of insufficient experimental data for these reactions.

One other point is noteworthy, that being the univariant reaction line "e" in Figure 15. The univariant line in the diagram will shift toward lower temperatures if  $P_f$  is less than  $P_{tot}$ , and if  $P_{CO_2}$  is present in any abundance. In the study area, it is not really decipherable how closely  $P_{H_2O}$  approached  $P_f$ .  $P_{CO_2}$  probably played an important role because calcite is ubiquitous in the area. Nearly all of the metamorphic minerals are hydrous, so  $P_{H_2O}$  was certainly high. Therefore, using Liou's diagram as it is in Figure 15, Table 11 shows the relationship between pressure and thickness of the overlying rock column which produced the pressures, assuming that  $P_{H_2O} = P_{tot}$ . To find these values of thickness, the formula  $P = \rho gh$  was used; where  $P$  = pressure, read from Liou's diagram;  $\rho$  = density of basalt, which Halls (1969) found to lie between 2.93 and 2.99 gm/cm<sup>3</sup> for amphibole-bearing (actinolitic) basalts in the Lake Superior area;  $g$  is the acceleration due to gravity; and  $h$  is the thickness of the overlying pile of lavas. In order to reasonably estimate the thickness, it should be noted that Grout et al (1951) indicated that there is probably a total thickness of 30,000 feet of basalts along the North Shore of Lake Superior. Sandberg (1938), indicates that about 13,500 feet of gabbro overlies the basal flows. This places a maximum of roughly 44,000 feet of overlying rock on the Ely's Peak basalts,

including the Duluth Complex. This thickness easily supplies the needed pressures for the formation of wairakite. However, this thickness implies that the basalts were poured out in horizontal, uniform sheets and that the whole sequence was once overlying the Ely's Peak area. Because of low initial dips which the overlying flows and gabbro may have had, the total weight of the overlying rock was probably never directly on the basal flows, but only a portion of this total weight. It can be said, though, with reasonable certainty, that there must have been from about 20,000 to 25,000 feet of rock overlying the Ely's Peak area, corresponding to pressures between 2,000 and 2,500 bars.

| Lithostatic Pressure in Bars | Equivalent Thickness of Basalt<br>in Feet |
|------------------------------|---|
| 1,500                        | 15,500                                    |
| 2,000                        | 20,700                                    |
| 2,500                        | 26,000                                    |
| 3,000                        | 31,200                                    |

Table 11

Metamorphic temperatures of about 290° C to 370° C can be estimated from Liou's experimental work (Figure 15). If it can be assumed that the same geothermal gradient existed then as does now, i.e. about 30° C/km, then, assuming 0° C at the surface, at depths of 20,000 to 25,000 feet, the temperature would lie between 210° C and 255° C. If  $P_f = P_{tot}$ , then these temperatures would be too low to accomplish the observed metamorphic effects. In addition to the above P-T estimations, the temperatures of metamorphism could also be estimated from opaque mineral alteration as observed by Hubbard, Palmer, and Ade-Hall (1971). The alteration of the opaques appears to correspond to the class 3,

Type I of Hubbard and others (1971) which they indicate takes place at temperatures of about 300° C. This temperature, then, could be a close approximation of the temperatures during metamorphism.

It should be noted that it is not really known when, if at all, the hydrothermal alteration took place relative to completion of the lava pile. If the alteration is regional, it should have taken place prior to intrusion of the Duluth Complex. If the Duluth Complex superimposed a contact metamorphism on the regional metamorphism, then this regional metamorphism cannot be distinguished with absolute certainty from the outer zones of contact metamorphism (albite-epidote-hornfels). The key, perhaps, lies outside the zone of contact metamorphism where primary igneous textures are still preserved. However, no solution can be derived from these flows since the mineral assemblages for both the greenschist facies and the albite-epidote-hornfels facies are the same, and since there was no deformation to produce a metamorphic foliation during regional metamorphism. Therefore, the strongest argument for regional metamorphism could be in the regional metamorphism developed in the flows near Leif Ericson Park directly over the Ely's Peak basalts and Duluth Gabbro in the City of Duluth and in the zeolitic alteration in the entire overlying part of the North Shore Volcanic Group. At Leif Ericson Park, the flows have been regionally metamorphosed to the zeolite to greenschist facies. If the flows near Leif Ericson Park had, at one time, directly overlain the Ely's Peak basalts, and since they are regionally metamorphosed, then it is most likely that the Ely's Peak basalts were also regionally metamorphosed.

This regional metamorphism probably took place prior to the intrusion of the Duluth Complex at temperatures of up to 260° C. When



the gabbro intruded, it probably elevated the temperatures to 290° C to 370° C and thus permitted the formation of wairakite and superimposing a contact-metamorphism on the regional metamorphism. The already formed greenschist minerals, i.e. albite, actinolite, epidote, and chlorite were apparently perfectly compatible with these raised temperatures because these minerals persisted outside the 250 to 300 yard wide contact zone.

## GEOLOGIC HISTORY

During the latter portion of Animikian time in the Middle Precambrian, sedimentation in the area of what is now southwestern St. Louis County produced a sequence of intercalated graywackes, siltstones, and shales to a total thickness of at least 3,000 feet (Wright, Mattson and Thomas, 1970). This sequence, known as the Thomson Formation, along with earlier deposition of iron formation further to the north in the vicinity of the Mesabi Range and to the west in the Cuyuna Range, took place in a slowly subsiding trough. Middle Precambrian time ended with the Penokean orogeny which took place about 1.8 billion years ago (Goldich, 1972) along a northeast-southwest linear trend across the southern part of the Lake Superior region. Included in this orogeny was the deformation of the Thomson Formation; the sediments were folded and altered to slates, metagraywackes, and metasiltstones of the greenschist facies. The deformation served to fold the Thomson Formation isoclinally with nearly vertical axial planes trending approximately east-west.

After deformation and erosion of the Thomson Formation, about six hundred million years elapsed during which no deposition occurred. Then, in Lower Keweenawan time, in the area near Nopeming, a quartz sandstone was deposited with angular unconformity on the Thomson Formation. At approximately the same time, deposition of similar quartz sandstone took place elsewhere in the Lake Superior region, for instance at Grand Portage, Minnesota (Puckwunge Formation). Mattis (1972) concludes that the sandstone at Nopeming is not correlative with the

Puckwunge Formation. He bases this hypothesis on presence of sandstone xenoliths in the lowermost flow at Grand Portage, indicating that the sandstone was lithified when the lavas were deposited over it. The sandstone at Nopeming is squeezed up between the pillows in the overlying flow, indicating soft-sediment deformation. This indicates that the sandstone was unlithified when the flows were deposited. At Nopeming, the flows were deposited conformably over the sandstone while at Grand Portage a slight unconformity exists between sandstone and overlying lava. The flows in these two areas were both deposited during the same period of reversed magnetic polarity (Green and Books, 1972). However, there is no evidence to indicate that the basal flows at the two localities were extruded contemporaneously.

Since only a total thickness of 25 to 28 feet of sandstone is present at Nopeming, the period of sandstone deposition was probably of short duration. If the Continental Rift hypothesis of Smith, Steinhart, and Aldrich (1966) and of Davidson and others (1971) is accepted as an explanation for the ensuing tectonic and igneous activity in the Lake Superior region, then the following could have happened. The western Lake Superior region became tectonically unstable and rift formation initiated by plate splitting took place with subsequent upwelling of low velocity layer material into the upper mantle along the base of the crust (Davidson and others, 1971). The effect of this upwelling was to produce a rising body of magma caused by partial melting and fractionation. The rising magma body caused uplift and igneous activity at the earth's surface along northeast trending zones of weakness. This igneous activity produced the North Shore Volcanic group and the Duluth Complex.

The lavas at Nopeming were probably extruded in rapid succession because there is a complete absence of any soil horizons, and interflow sediments are very minor. From his studies of the volcanics along the North Shore, Sandberg (1938) believed the entire sequence to have been deposited in a short time, geologically speaking. Green and Silver (1963) obtained U-Pb age dates of about 1,115 million years from the middle Keweenawan igneous rocks of the Lake Superior region. They indicate that because of a very limited time spread of cogenetic zircons used for age dating, a sharp pulse of igneous activity must have occurred. After deposition of the North Shore volcanics and subsequent intrusion of the Duluth Complex in Middle Keweenawan time, the residual molten low velocity layer of the mantle began to cool. As it cooled, the mantle deflated. This deflation placed the crust into a state of compression which accounts for the compressional features associated with the rift system, and also the development of the Middle Keweenawan Lake Superior syncline (Davidson and others, 1971). This deflating is manifested on the surface by the 5 to 20 degree dip of the flows toward the Lake.

While the North Shore Volcanics were filling the trough during Middle Keweenawan time, the Ely's Peak basalts, at the base, were being buried and hydrothermally metamorphosed. Later, when the Duluth Gabbro Complex intruded, it contact-metamorphosed the Ely's Peak basalts to a granofels for a distance of up to one-fifth of a mile from the contact.

Sometime after the Ely's Peak basalts had been deposited, they were intruded by a swarm of mafic dikes that followed about a N 30° E joint set. These dikes were also low-grade metamorphosed.

In Upper Keweenawan time, along the St. Louis River near Fond du Lac, sedimentation occurred over the lavas producing at least 800 feet



of lenticular beds of red sandstone, siltstone, and conglomerate. This is known as the Fond du Lac Formation (Morey, 1967). Analysis of cross-bedding and other sedimentary directional indicators imply that the formation was derived from a terrane consisting of igneous, high-grade metamorphic, and sedimentary rocks that probably was situated to the west of the Fond du Lac basin of deposition (Morey, 1967).

After deposition of the Fond du Lac Formation, tilting occurred in the western Lake Superior region followed by a long hiatus, from Upper Keweenawan time until Pleistocene time, during which there was no recorded sedimentation in the Duluth area. Then, during Pleistocene time, glaciers advanced over the area, scouring the rocks in their path. The Ely's Peak basalts show glacial grooving on many outcrop surfaces, as do most of the rocks in the Duluth area. Upon melting, the glaciers left a weak terminal moraine and ground moraine in the northern portion of the subject area. Glacial Lake Duluth clays were deposited in the southern portion of the map area and this clay has since been deeply eroded by streams that drain via the St. Louis River into Lake Superior.

## CONCLUSIONS

As a result of this study, the Ely's Peak basalts have been found to consist of both alkali and tholeiite basalts. There are a minimum of 20 flows with a total thickness of about 1,200 feet. The flows dip east toward Lake Superior at angles of  $5^{\circ}$  to  $20^{\circ}$ .

The Ely's Peak basalts have undergone at least one, and probably two, periods of metamorphism. It is thought that the flows underwent regional hydrothermal metamorphism due to burial, and later, contact metamorphism may have been superimposed on the earlier metamorphism by intrusion of the Duluth Gabbro Complex. It should be pointed out that it is very difficult to firmly establish if there ever really was an earlier hydrothermal metamorphism from evidence within the study area.

Because of the distinctive pyroxene-porphyrific flows at the base of the Ely's Peak basalts and at the base of the Grand Portage lavas on Lucille Island, near Grand Portage, Minnesota, and because the basal flows in these two areas were found to have reversed magnetic polarity, they are thought to correlate in general time of deposition and in physical conditions of magma generation.

APPENDIX A

Data On Wairakite

Physical and Optical Properties

$\text{CaAl}_2\text{Si}_4\text{O}_{12}\cdot 2\text{H}_2\text{O}$  -- Monoclinic

Color: Pinkish orange - colorless to pale orange in thin section  
 Luster: Non-metallic  
 Streak: White  
 Cleavage: Imperfect in one direction  
 Hardness: 5 - 5-1/2  
 Density: 2.25  
 Form: Irregular blocky masses  
 Relief: Moderate, n less than balsam  
 Birefringence: Nil to very weak - up to first order gray to white  
 Extinction: Slightly inclined  
 Optic Angle: Large, variable 2V  
 Other Properties: Contains polysynthetic twins and often looks very cloudy in plane light

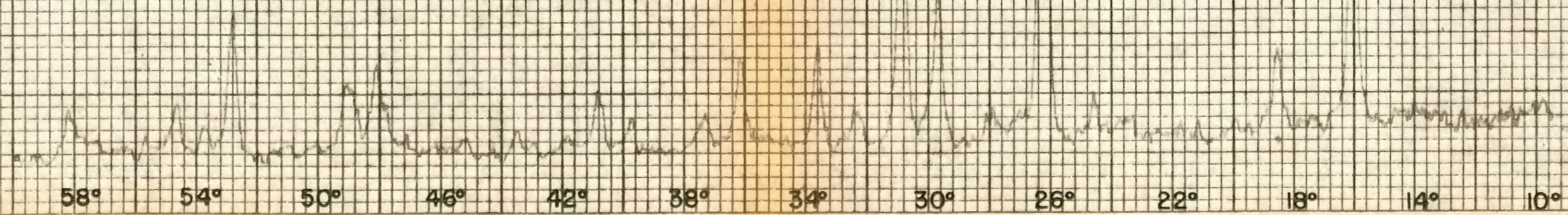
X-Ray Data -  $\text{CuK}_\alpha$  Radiation

| $2\theta$ | $d\text{\AA}$ | I   |
|-----------|---------------|-----|
| 15.95     | 5.56          | 54  |
| 18.35     | 4.80          | 21  |
| 24.45     | 3.64          | 6   |
| 26.10     | 3.42          | 100 |
| 30.75     | 2.907         | 55  |
| 32.20     | 2.78          | 6   |
| 33.45     | 2.67          | 16  |
| 36.04     | 2.49          | 16  |
| 37.20     | 2.42          | 8   |
| 39.60     | 2.27          | 4   |
| 40.70     | 2.218         | 10  |
| 43.50     | 2.08          | 4   |
| 47.00     | 1.936         | 4   |
| 48.10     | 1.89          | 14  |
| 49.00     | 1.85          | 10  |
| 52.65     | 1.74          | 18  |
| 53.70     | 1.707         | 4   |
| 54.50     | 1.68          | 4   |
| 57.20     | 1.61          | 2   |
| 58.00     | 1.59          | 9   |



Figure 16

X-RAY PATTERN OF WAIRAKITE  
 $\text{CuK}\alpha - 4^\circ 2\theta$



58° 54° 50° 46° 42° 38° 34° 30° 26° 22° 18° 14° 10°



## REFERENCES

- Ade-Hall, J. M., Palmer, H. C. and Hubbard, T. P., 1971, The Magnetic and Opaque Petrological Response of Basalts to Regional Hydrothermal Alteration: *Geophys. J. R. Astr. Soc.*, V. 24, pp. 137-174.
- Carmichael, I. S. E., 1964, The Petrology of Thingmuli, A Tertiary Volcano in Eastern Iceland: *Jour. of Petrology*, V. 5, pp. 435-460.
- Davidson, D. M., Hinze, W. J., and Roy, R. F., 1971, Continental Rifts: 17th Annual Institute on Lake Superior Geology (abs.), p. 29.
- Deer, Howie and Zussman, 1967, *Rock Forming Minerals*: V. 2 and 4, Longmans, Green and Co. Ltd., London.
- Goldich, S. S., 1972, The Penokean Orogeny: 18th Annual Institute on Lake Superior Geology (abs.), paper #25.
- Goldich, S. S., Nier, A. O., Baadsgaard, H., Hoffman, J. H. and Krueger, H. W., 1961, The Precambrian Geology and Geochronology of Minnesota: *Minn. Geol. Survey Bull.* 41, 193 p.
- Green, J. C., 1972, North Shore Volcanic Group and Associated Minor Intrusions: in *Geology of Minnesota Centennial Volume*, University of Minnesota Press.
- Green, J. C., 1971, Stratigraphy of the North Shore Volcanic Group Northeast of Silver Bay, Minn.: 17th Annual Institute on Lake Superior Geology (abs.), p. 20.
- Green, J. C., 1968, Varieties of Flows in the North Shore Volcanic Group, Minnesota: 14th Annual Institute on Lake Superior Geology, 5 p.
- Green, J. C. and Books, K. G., 1972, Paleomagnetic Evidence for the Extent of Lower Keweenaw Lavas in Minnesota: 18th Annual Institute on Lake Superior Geology (abs.), paper #8.
- Green, J. C. and Silver, L. T., 1963, Zircon Ages for Middle Keweenaw Rocks of the Lake Superior Region: *Am. Geophys. Union Trans.*, V. 44, p. 107.
- Green, T. H., Green, D. H., and Ringwood, A. E., 1967, The Origin of High-Alumina Basalts and Their Relationships to Quartz Tholeiites and Alkali Basalts: *Earth and Planetary Science Letters*, V. 2, pp. 41-51.

- Grout, F. F., Gruner, J. W., Schwartz, G. M., and Thiel, G. A., 1951, Precambrian Stratigraphy of Minnesota: G.S.A. Bull., V. 62, pp. 1017-1078.
- Halls, H. C., 1969, Compressional Wave Velocities of Keweenaw Rock Specimens From the Lake Superior Region: Can. Jour. Earth Sci., V. 6, no. 2, pp. 555-568.
- Heinrich, W. E., 1965, Microscopic Identification of Minerals: McGraw-Hill Book Co., Inc., New York.
- Hubbard, N. J., Meyer, C., Jr., Gast, P. W., and Wiesmann, H., 1971, The Composition and Derivation of Apollo 12 Soils: Earth and Planetary Science Letters, V. 10, pp. 341-350.
- Kuno, H., 1960, High Alumina Basalt: Jour. of Petrology, V. 1, pp. 121-145.
- Liou, J. G., 1970b, Synthesis and Stability Relations of Wairakite  $\text{CaAl}_2\text{Si}_4\text{O}_{12}\cdot 2\text{H}_2\text{O}$ : Contr. Mineral. and Petrol., V. 27, pp. 259-282.
- Liou, J. G., 1971, P-T Stabilities of Laumontite, Wairakite, Lawsonite, and Related Minerals in the System  $\text{CaAl}_2\text{Si}_2\text{O}_8 - \text{SiO}_2 - \text{H}_2\text{O}$ : Jour. of Pet., V. 12, no. 2, pp. 379-411.
- Liou, J. G., 1971, Stilbite-Laumontite Equilibrium: Contr. to Mineral. And Petrol., V. 31, no. 3, pp. 171-177.
- Liou, J. G., 1971, Synthesis and Stability of Prehnite  $\text{Ca}_2\text{Al}_2\text{Si}_3\text{O}_{10}(\text{OH})_2$ : The Am. Mineralogist, V. 56, nos. 3-4, pp. 507-531.
- MacDonald, G. A. and Katsura, T., 1964, Chemical Compositions of Hawaiian Lavas: Jour. of Petrology, V. 5, pp. 82-133.
- Mattis, A. F., 1972, The Petrology and Sedimentation of the Basal Keweenaw Sandstones of the North and South Shores of Lake Superior: Unpublished Master's Thesis, University of Minnesota, Duluth.
- Morey, G. B., 1967, Stratigraphy and Petrology of the Type Fond du Lac Formation, Duluth, Minnesota: Minnesota Geological Survey Report of Investigation 7, 35 p.
- Morey, G. B. and Ojakangas, R. W., 1970, Sedimentology of the Middle Precambrian Thomson Formation, East-Central Minnesota: Minnesota Geological Survey Report of Investigation 13, 32 p.
- Sandberg, A. E., 1938, Section Across Keweenaw Lavas at Duluth, Minnesota: G.S.A. Bull., V. 49, pp. 795-830.
- Schmincke, Hans-Ulrich, 1967, Stratigraphy and Petrography of Four Upper Yakima Basalt Flows in South-Central Washington: G.S.A. Bull., V. 78, pp. 1385-1422.

- Schwartz, G. M., 1949, The Geology of the Duluth Metropolitan Area: Minnesota Geological Survey Bull. 33, 136 p.
- Seki, Y., 1966, Wairakite in Japan: J. Japanese Assoc. Mineral. Petrol. Econ. Geol., V. 56, pp. 254-261, 30-39.
- Smith, T. J., Steinhart, J. S., and Aldrich, L. T., 1966, Lake Superior Crustal Structure: Jour. of Geophys. Research, V. 71, no. 4, pp. 1141-1172.
- Swanson, D. A., 1967, Yakima Basalt of the Tieton River Area, South-Central Washington: G.S.A. Bull., V. 78, pp. 1077-1110.
- Taylor, R. B., 1964, Geology of the Duluth Gabbro Complex near Duluth, Minnesota: Minnesota Geological Survey Bull. 44, 63 p.
- Turner, F. J., 1968, Metamorphic Petrology: McGraw-Hill Book Co., Inc., New York.
- Turner, F. J. and Verhoogen, J., 1960, Igneous and Metamorphic Petrology: McGraw-Hill Book Co., Inc., New York.
- Wager, L. R., 1960, The Major Element Variation of the Layered Series of the Skaergaard Intrusion and a Re-Estimation of the Average Composition of the Hidden Layered Series and of Successive Residual Magmas: Jour. of Petrology, V. 1, pp. 364-398.
- Whetten, J. T., 1965, Wairakite from Low-Grade Metamorphic Rocks on St. Croix, U.S. Virgin Islands: Am. Mineralogist, V. 50, pp. 752-755.
- White, W. S., 1966, Tectonics of the Keweenaw Basin, Western Lake Superior Region: USGS Prof. Paper 524-E, 23 p.
- White, W. S., 1960, The Keweenaw Lavas of Lake Superior, an Example of Flood Basalts: Am. Jour. Sci., Bradley Volume, V. 258-A, pp. 367-374.
- Winchell, N. H., 1899, Geology of Minnesota: Minnesota Geological Survey Final Report, V. IV, 630 p.
- Wise, W. S., 1959, Occurrence of Wairakite in Metamorphic Rocks of the Pacific Northwest: Am. Mineralogist, V. 44, pp. 1099-1101.
- Wright, H. E., Mattson, L. A., and Thomas, J. A., 1970, Geology of the Cloquet Quadrangle, Carlton Co., Minnesota: Minnerota Geological Survey, Map Series 3, 30 p.
- Yoder, H. S., Jr., and Tilley, C. E., 1962, Origin of Basaltic Magmas: An Experimental Study of Natural and Synthetic Rock Systems: Jour. of Petrology, V. 3, pp. 342-532.